Molecular Cancer Therapeutics

Structure-Based Screen Identifies a Potent Small Molecule Inhibitor of Stat5a/b with Therapeutic Potential for Prostate Cancer and Chronic Myeloid Leukemia

Zhiyong Liao[1], Lei Gu[1], Jenny Vergalli[1], Samanta A. Mariani[1], Marco De Dominici[1], Ravi K. Lokareddy[2], Ayush Dagvadorj[1], Puranik Purushottamachar[3], Peter A. McCue[4], Edouard Trabulsi[5], Costas D. Lallas[5], Shilpa Gupta[1,6], Elyse Ellsworth[1], Shauna Blackmon[1], Adam Ertel[1], Paolo Fortina[1], Benjamin Leiby[7], Guanjun Xia[1], Hallgeir Rui[1,4,6], David T. Hoang[1], Leonard G. Gomella[5], Gino Cingolani[2], Vincent Njar[3], Nagarajan Pattabiraman[1,8], Bruno Calabretta[1], and Marja T. Nevalainen[1,5,6]

Abstract

Bypassing tyrosine kinases responsible for Stat5a/b phosphorylation would be advantageous for therapy development for Stat5a/b-regulated cancers. Here, we sought to identify small molecule inhibitors of Stat5a/b for lead optimization and therapy development for prostate cancer and Bcr-Abl–driven leukemias. *In silico* screening of chemical structure databases combined with medicinal chemistry was used for identification of a panel of small molecule inhibitors to block SH2 domain–mediated docking of Stat5a/b to the receptor-kinase complex and subsequent phosphorylation and dimerization. We tested the efficacy of the lead compound IST5-002 in experimental models and patient samples of two known Stat5a/b-driven cancers, prostate cancer and chronic myeloid leukemia (CML). The lead compound inhibitor of Stat5-002 (IST5-002) prevented both Jak2 and Bcr-Abl–mediated phosphorylation and dimerization of Stat5a/b, and selectively inhibited transcriptional activity of Stat5a (IC_{50} = 1.5μmol/L) and Stat5b (IC_{50} = 3.5 μmol/L). IST5-002 suppressed nuclear translocation of Stat5a/b, binding to DNA and Stat5a/b target gene expression. IST5-002 induced extensive apoptosis of prostate cancer cells, impaired growth of prostate cancer xenograft tumors, and induced cell death in patient-derived prostate cancers when tested *ex vivo* in explant organ cultures. Importantly, IST5-002 induced robust apoptotic death not only of imatinib-sensitive but also of imatinib-resistant CML cell lines and primary CML cells from patients. IST5-002 provides a lead structure for further chemical modifications for clinical development for Stat5a/b-driven solid tumors and hematologic malignancies. *Mol Cancer Ther; 14(8); 1777–93. ©2015 AACR.*

[1]Department of Cancer Biology, Sidney Kimmel Cancer Center, Thomas Jefferson University, Philadelphia, Pennsylvania. [2]Department of Biochemistry, Sidney Kimmel Cancer Center, Thomas Jefferson University, Philadelphia, Pennsylvania. [3]School of Pharmacy, Sidney Kimmel Cancer Center, Thomas Jefferson University, Philadelphia, Pennsylvania. [4]Department of Pathology, Sidney Kimmel Cancer Center, Thomas Jefferson University, Philadelphia, Pennsylvania. [5]Department of Urology, Sidney Kimmel Cancer Center, Thomas Jefferson University, Philadelphia, Pennsylvania. [6]Department of Medical Oncology, Sidney Kimmel Cancer Center, Thomas Jefferson University, Philadelphia, Pennsylvania. [7]Division of Biostatistics, Department of Pharmacology and Experimental Therapeutics, Sidney Kimmel Cancer Center, Thomas Jefferson University, Philadelphia, Pennsylvania. [8]Department of Oncology, Lombardi Comprehensive Cancer Center, Georgetown University, Washington, District of Columbia.

Note: Supplementary data for this article are available at Molecular Cancer Therapeutics Online (http://mct.aacrjournals.org/).

Current address for V. Njar and Puranik Purushottamachar: University of Maryland School of Medicine, 685 West Baltimore Street, HSF 1, Suite 580E, Baltimore, Maryland; and current address for Shilpa Gupta, Medical Oncology, Moffitt Cancer Center, 12902 Magnolia Drive, Tampa, Florida.

Corresponding Author: Marja T. Nevalainen, Translational and Biomedical Research Center, C4980, Cancer Center of Medical College of Wisconsin, 8701 Watertown Plank Rd., Milwaukee, WI 53226. Phone: 301-219-6689; E-mail: mnevalainen@mcw.edu

doi: 10.1158/1535-7163.MCT-14-0883

Introduction

There is an unmet medical need for pharmacologic inhibitors of signal transducer and activator of transcription 5a/b (Stat5a/b). Stat5a/b is critical for growth and progression of solid tumors and hematologic malignancies, specifically prostate cancer (1–9) and Bcr-Abl–driven leukemias (10–19), respectively. In prostate cancer, effective therapeutic options are lacking for advanced castrate-resistant prostate cancer (CRPC), for which Stat5a/b is an experimentally established therapeutic target candidate (2, 4, 9, 20, 21). Multiple findings support Stat5a/b as a therapeutic target protein in prostate cancer: (i) inhibition of Stat5a/b expression or activation induces rapid apoptotic prostate cancer cell death (1–3, 9, 22); (ii) blockade of Stat5a/b signaling inhibits growth of both primary prostate cancer and CRPC (2, 4, 5, 9, 21–23); (iii) Stat5a/b promotes epithelial–mesenchymal transition (EMT) and metastasis of human prostate cancer (5); (iv) the Stat5a/b gene locus is frequently amplified in clinical prostate cancers during progression to metastatic CRPC (6); (v) Stat5a/b activation in prostate cancer predicts early recurrence and prostate cancer–specific death (7, 8, 21).

Chronic myeloid leukemia (CML) is a clonal hematopoietic stem cell malignancy characterized by the unique t(9:22) (q34:q11) translocation, which generates the *BCR-ABL* oncogene (24).

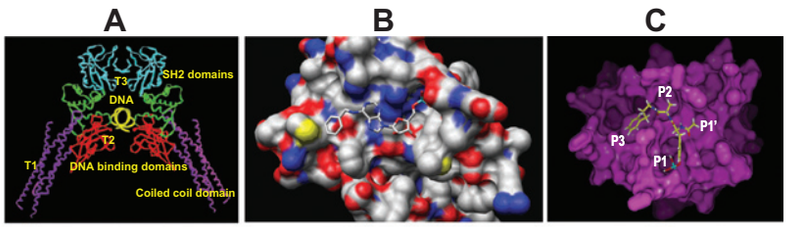
A
B
C
SH2 domains
T3
DNA
T2
T1
DNA binding domains
Coiled coil domain
P2
P1'
P3
P1

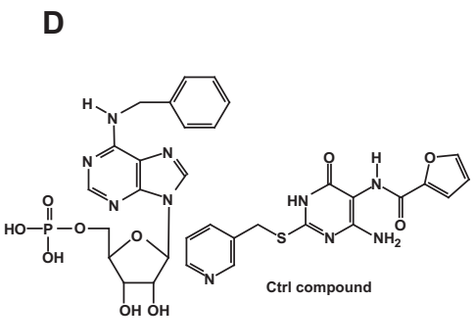
D
IST5-002
Stat5a: IC50=1.5 μmol/L
Stat5b: IC50=3.5 μmol/L
Ctrl compound

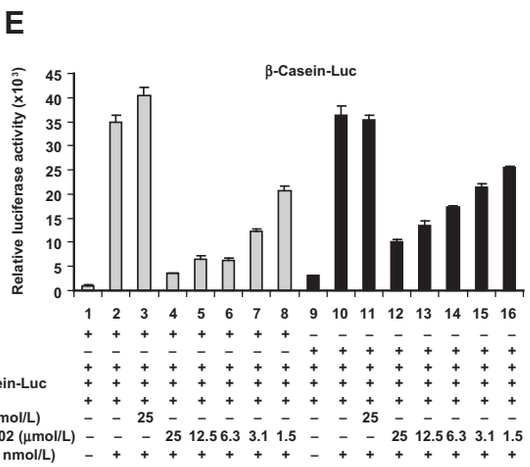
E
β-Casein-Luc
Relative luciferase activity (x10³)
Stat5a
Stat5b
PrlR
β-Casein-Luc
RL
Ctrl (μmol/L)
IST5-002 (μmol/L)
Prl (10 nmol/L)

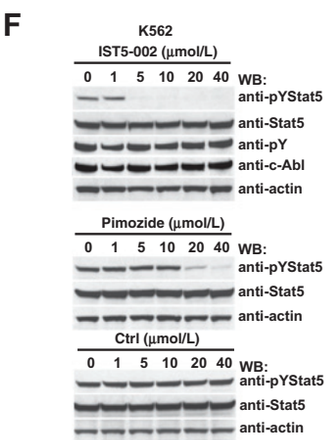
F
K562
IST5-002 (μmol/L)
Pimozide (μmol/L)
Ctrl (μmol/L)
WB:
anti-pYStat5
anti-Stat5
anti-pY
anti-c-Abl
anti-actin

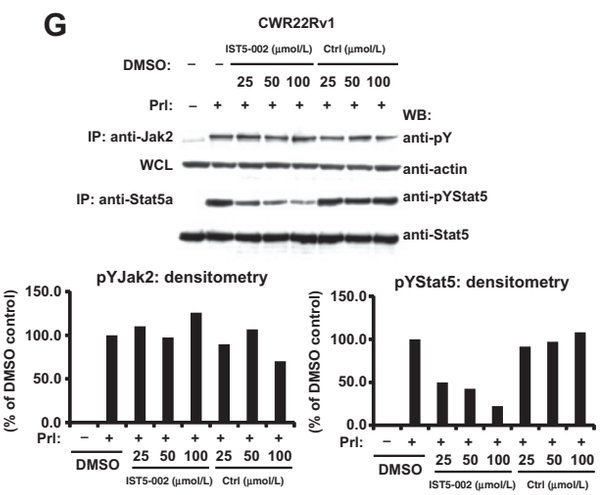
G
CWR22Rv1
DMSO:
IST5-002 (μmol/L)
Ctrl (μmol/L)
Prl:
IP: anti-Jak2
WCL
IP: anti-Stat5a
WB:
anti-pY
anti-actin
anti-pYStat5
anti-Stat5
pYJak2: densitometry
pYStat5: densitometry
(% of DMSO control)

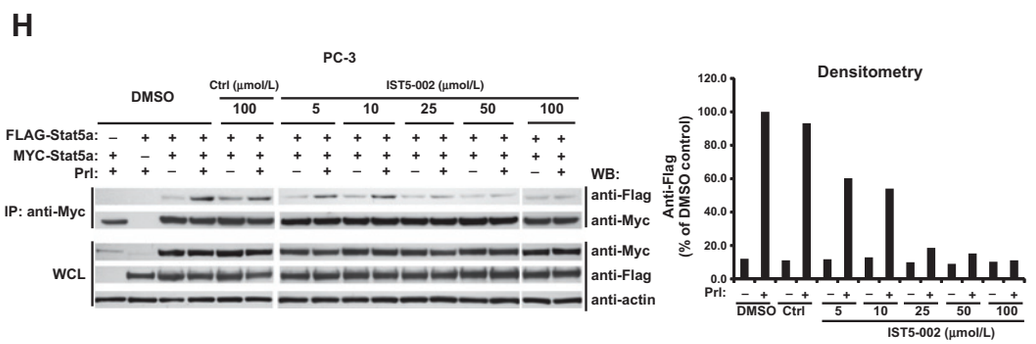
H
PC-3
DMSO
Ctrl (μmol/L)
IST5-002 (μmol/L)
FLAG-Stat5a:
MYC-Stat5a:
Prl:
IP: anti-Myc
WCL
WB:
anti-Flag
anti-Myc
anti-actin
Densitometry
Anti-Flag
(% of DMSO control)

Bcr-Abl is a constitutively active tyrosine kinase promoting transformation, proliferation, and survival of CML cells via Stat5a/b signaling (10–19, 25). Resistance to the predominant pharmacologic inhibitor of Bcr-Abl, imatinib mesylate (Gleevec; ref. 26), induced by point mutations within the Abl kinase domain or overexpression of Bcr-Abl (27, 28), is, in part, dependent on activation of the Stat5a/b signaling pathway (10, 14, 18).

Stat5a/b includes two highly homologous isoforms Stat5a and Stat5b (hereafter referred to as Stat5a/b), which display >90% amino acid identity and are encoded by genes juxtaposed on chromosome 17q21.2 (29). Stat5a/b are latent cytoplasmic proteins that function as both signaling proteins and nuclear transcription factors. Activation of Stat5a/b occurs through inducible phosphorylation of a conserved C-terminal tyrosine residue (29). Phosphorylated Stat5a/b (pY694/699) molecules form functional parallel dimers that translocate to the nucleus and bind specific DNA response elements (29). Stat5a/b proteins comprise five functional domains: (i) N-terminal domain (29); (ii) coiled-coil domain (30); (iii) DNA-binding domain (29); (iv) Src-homology 2 (SH2) domain, which mediates receptor-specific recruitment and Stat5a/b dimerization (29); and (v) C-terminal transactivation domain (29). In prostate cancer, Stat5a/b is activated by the upstream kinase Jak2 and by other tyrosine kinases such as Src and growth factor receptors (31–34). In CML, Stat5a/b is phosphorylated directly by Bcr-Abl (35) and targeting Stat5a/b would bypass Bcr-Abl and might provide an effective therapy especially in imatinib-resistant CML (10–19, 25). Therefore, targeting of Stat5a/b as a cytoplasmic signaling protein in both prostate cancer and CML may prove a more effective therapeutic strategy than inhibiting Stat5a/b tyrosine kinases.

In this study, we identified a small molecule inhibitor family of Stat5a/b through structure-based *in silico* screening and medicinal chemistry by targeting the Stat5a/b SH2 domain. The SH2 domain of a Stat5 monomer docks transiently to a phospho-tyrosyl moiety of a tyrosine kinase complex, which facilitates phosphorylation of Y694/699 residue of Stat5a/b. The SH2 domain of each phosphorylated Stat5 monomer forms transcriptionally active parallel dimers through binding of pY694/699 residue of the partner Stat5 monomer (36). Therefore, a small molecule that interferes with the SH2 domain should inhibit both Stat5a/b phosphorylation and dimerization. Our lead compound, inhibitor of Stat5-002 (IST5-002) blocked both Jak2 and Bcr-Abl–mediated phosphorylation of Stat5a/b and disrupted dimerization, nuclear translocation, DNA binding, and transcriptional activity. IST5-002 induced apoptotic death of prostate cancer cells and imatinib-sensitive and -resistant CML cells *in vitro*. Furthermore, IST5-002 inhibited growth of prostate cancer xenograft tumors *in vivo* and Stat5a/b-positive patient-derived prostate cancers in *ex vivo* organ culture. These findings establish a potent small molecule Stat5a/b inhibitor compound for further optimization and therapy development for prostate cancer and Bcr-Abl–driven leukemias.

Materials and Methods

Discovery of small molecule Stat5 inhibitor IST5-002 through *in silico* database screen

To identify candidate compounds that disrupt Stat5a/b dimerization by targeting the SH2 domain, we created a three-dimensional model of the SH2 domain dimer structure (amino acid residues 589-710) of human Stat5b using the homology modeling software, MODELLER 6v2. The sequence of the human Stat5b SH2 domain with an additional 14 amino acids (697-DGYVKPQIKQVVPE-710) at the C-terminus, containing the phosphotyrosine (UniProtKB/Swiss-Prot ID:P51692), was used to search for sequences that matched the sequences of three-dimensional structures of proteins and their complexes available in the Protein Data Bank using BLAST (National Center for Biological Information). The sequence homology between human *STAT5A* and *STAT5B* is approximately 92%, whereas the sequence homology between the SH2 domains of human *STAT5A* and *STAT5B* is approximately 98% (29). We identified two protein structures: (i) Stat3–DNA complex (PDB ID: 1BG1; ref. 30), with identities equal to 35%, positives equal to 11%, and gaps equal to 53%); and (ii) tyrosine-phosphorylated Stat1–DNA complex (PDB ID: 1BF5; ref. 37), with identities equal to 56%, positives equal to 34%, and gaps equal to 12%) with expected values (e-value) of 9e−14 and 7e−12, respectively. By aligning the sequences between the SH2 domains of human *STAT5B* and *STAT3* and using the crystal structure of the SH2 domain of the Stat3–DNA complex as a template, a homology model of the SH2 domain of human Stat5b was built. This homology model was further energy-minimized until the root-mean-square deviation was < 0.09 using AMBER7 (UCSF) and its force field with a distance-dependent dielectric constant. To perform structure-based *in silico* screening, the pY binding subpocket is insufficient to identify

Figure 1.
Identification and functional characterization of the Stat5a/b inhibitor IST5-002. A, ribbon presentation of the crystal structure of Stat–DNA complex and the various functional domains are labeled. Predicted binding model of IST5-002 to the Stat5a SH2 domain, shown as atom-based (carbon, white; oxygen, red; nitrogen, blue; phosphorous, cyan; sulfur, yellow) bonds within the binding site at the SH2 dimer interface (B), and by stick model, depicting the SH2 dimer interface site of Stat5a (magenta) with labeled subpockets P1, P2, P3, and P1′ of the SH2 interface (C). D, chemical structures of the Stat5a/b inhibitor IST5-002 and the control compound (Ctrl) with similar molecular weight as IST5-002. E, IST5-002 inhibits transcriptional activity of Stat5a/b. PC-3 cells were transiently cotransfected with a β-casein-promoter-luciferase plasmid, pRL-TK (*Renilla* luciferase), pPrl-receptor (PrlR), pStat5a or pStat5b, as indicated. Cells were serum starved (0% FBS; 10 hours) and pretreated with IST5-002 or Ctrl at the indicated concentrations (2 hours), followed by stimulation with 10 nmol/L human prolactin (hPrl; 16 hours). Relative luciferase activities were determined, and mean values of three independent experiments performed in triplicate ± SE values are indicated by bars. F and G, IST5-002 inhibits Bcr-Abl–driven (F) and Jak2-driven (G) Stat5 phosphorylation. Whole-cell lysates of exponentially growing K562 cells and Stat5a/b immunoprecipitates of CWR22Rv1 cells were immunoblotted with anti-pYStat5 mAb, anti-Stat5a/b mAb, anti-pY mAb (for Jak2), anti-c-Abl pAb, or anti-actin pAb as loading control. In CWR22Rv1 cells, Stat5 and Jak2 were immunoprecipitated using anti-Stat5a or anti-Jak2 pAbs from serum-starved CWR22Rv1 cells (16 hours), treated with IST5-002 (2 hours), followed by stimulation with 10 nmol/L hPrl (30 minutes). H, IST5-002 suppresses Stat5 dimerization. pCMV-3Flag-Stat5a, pCMV-3Mys-Stat5a, and pPrlR plasmids were cotransfected into PC-3 cells. Cells were serum-starved (16 hours), pretreated with IST5-002 or Ctrl at indicated concentrations (2 hours), followed by stimulation with 10 nmol/L hPrl (30 minutes). 3-Myc-Stat5a was immunoprecipitated with anti-Myc mAb and blotted with anti-Flag mAb or anti-Myc mAb, as indicated. Whole-cell lysates were blotted with anti-Myc, anti-Flag mAb, or anti-actin pAb to demonstrate the input.

Table 1. Prostate cancers cultured *ex vivo* in explant organ cultures

Age at the day of operation	Gleason grade	Gleason score	Stage	Nuclear Stat5 levels
58	(3+4)	7	T3a	3
66	(4+3)	7	T2b	3
72	(4+3)	7	T1c	3
55	(3+4)	7	T2b	3
66	(3+4)	7	T1c	2
60	(3+4)	7	T2a	2
55	(3+4)	7	T2a	3
67	(3+4)	7	T2a	2
50[a]	(3+4)	7	T2b	1
65[a]	(4+3)	7	T2c	1
66[a]	(4+3)	7	T3a	0

NOTE: Ages of the patients ranged from 50 to 72 years at the time of the operation (mean age 62 years).

[a]Prostate cancer samples that did not respond to IST5-002 by cancer cell death. Samples of each prostate cancer were scored for nuclear Stat5 levels on a scale from 0 to 3 where 0 represented negative, 1 weak, 2 moderate, and 3 strong immunostaining.

potent inhibitors against the dimer of SH2 domains, requiring additional two to three subpockets near the pY binding pocket. From analysis of the crystal structure of the Stat1–DNA complex at the SH2 dimer interface, it is clear that additional subpockets are available both at the N- and C-termini of the pY-binding site at the dimer interface. In order to identify these additional subpockets, 64 oligopeptides derived from the tetrapeptide sequence pYVKP (where pY is the phosphorylated tyrosine) by varying the amino acids to all eight hydrophobic/aromatic acids independently both at the second and fourth amino acid positions and docked into the binding site on the SH2 domain. By calculating the interaction energies of all 64 amino acids and rank-ordering them, we selected the following residues of Stat5b as the binding sites for *in silico* screening: 600K, 604H, 618-RFSDSEIGG-626, 628T, 638-RMFWNLMPF-646, 707-VVPE-710.

In silico screening of small organic molecules from databases (NCI, Maybridge, LeadQuest, Virtual Chemistry, and Drug-Like Compounds; http://www.chemnavigator.com) of 30 million compounds was performed against the subpockets at the dimer interface for their ability to disrupt Stat5b dimerization (Fig. 1A–C). We wanted to identify compounds that would mimic the side chain of pY and have additional groups occupying the subpockets described above. In our first-level search, we identified compounds with free phosphate group attached either to an aromatic or aliphatic five- or six-member ring. These compounds were screened against the phosphotyrosine-binding pocket using a flexible ligand docking program (FlexX module of Sybyl, Tripos) and multiple scoring functions (molecular mechanics energy, surface area, etc.), which led to the selection of the top-ranking 100 compounds. These compounds, along with their protein complexes, were energy-minimized using molecular mechanics CFF91 force-filed to better fit the ligands into the binding pocket. The top-ranking 30 small molecule inhibitors were selected from visual analysis of docking position and interactions to be further validated in biologic assays, and as the basis of the design and synthesis of compound analogs (Supplementary Fig. S1).

Cell lines and reagents

PC-3, DU145, and LNCaP prostate cancer cells, T47D breast cancer cells, and CML-cells (KCL22, K562, and BV173; all from ATCC in 2002), were cultured in RPMI-1640 (Mediatech) containing penicillin (50 IU/mL)/streptomycin (50 μg/ml; Mediatech), and 10% fetal bovine serum (FBS; Gemini BioProducts). CWR22Rv1 cells were provided by Dr. Thomas Pretlow (Case-western Reserve University, Cleveland, OH) in 2004. K562, imatinib-resistant K562 (K562R), BV173, imatinib-resistant-BV173 (BV173T315I) were maintained in Iscove's Modified Dulbecco's Medium (IMDM; Mediatech) supplemented with 1% penicillin/streptomycin, L-glutamine, and 10% FBS. KCL22R, K562R, and BV173R were kindly provided by Dr. Nicholas J. Donato (2009; University of Michigan, Ann Arbor, MI). SUP-B15, 12878, and 3798 (2009; Coriell Institute, Camden, NJ) were maintained in Iscove's medium with 10% FBS. LNCaP cells were supplemented with 0.5 nmol/L dihydrotestosterone (DHT; Sigma-Aldrich). CML $CD34^+$ cells from three CML patients (#3-342, #9537, and #3-295; 2010, a gift from Dr. Tessa Holyoake, University of Glasgow, Scotland, United Kingdom) were maintained in serum-free expansion medium (SFEM; STEMCELL Technologies) supplemented with 1% penicillin/streptomycin and L-glutamine (Gibco), a cytokine cocktail (100 ng/mL Flt3 ligand, 100 ng/mL SCF, 20 ng/mL interleukin (IL)-3, and 20 ng/mL IL6 (STEMCELL Technologies), and 100 ng/mL rhTPO (Prospec). Monkey kidney fibroblast (COS-7), human lung cancer (A549), fibrosarcoma (HT1080), pancreatic cancer (CAPAN), and liver cancer (HepG2) cell lines (all from ATCC in 2008) were grown in DMEM (Invitrogen) supplemented with 10% FBS, 2 mmol/L L-glutamine, and penicillin–streptomycin (Mediatech). All cell lines included in this study have been authenticated on a regular basis in the users' laboratory. The testing has been conducted by DNA fingerprinting, isozyme collection, observation of characteristic cell morphology, hormone/growth factor responsiveness, and the expression of cell lines specific markers such as prostate-specific antigen (PSA), hormone receptors, Stat3/Stat5, Erk1/2Protein, BCR-Abl. All cell lines were tested for *Mycoplasma* contamination (PCR Mycoplasma Detection Set; Takara Bio Inc.,) every 3 months. Pimozide was obtained from Sigma-Aldrich.

Luciferase reporter gene assays

PC-3 cells (2×10^5) were transiently cotransfected with 0.25 μg of pStat5a or pStat5b and pPrlR (prolactin receptor; PrlR), 0.5 μg of p-β-casein-luciferase (β-casein-Luc) and 0.025 μg of pRL-TK (*Renilla luciferase*). After 24 hours, cells were serum-starved for 10 hours, pretreated with compounds at indicated concentrations for 1 hour, and stimulated with 10 nmol/L human prolactin (hPrl) for 16 hours. For determination of Stat3 transcriptional activity, 0.25 μg of pcDNA-Stat3, 0.25 μg of pcDNA-IL6-R, 0.5 μg of pStat3-luciferase (Panomics), and 0.025 μg of pSV-β-Gal (Promega) were cotransfected to LNCaP cells, followed by serum-starvation and stimulation with 50 ng/mL IL6 (Prospec) for 16 hours. Cell lysates were assayed for firefly and *Renilla* luciferase activities using the Dual-Luciferase Reporter Assay System (Promega), as described previously (23).

Protein solubilization, immunoprecipitation, and immunoblotting

Cell pellets were immunoprecipitated and immunoblotted as described previously (2, 3, 5, 23). Stat5a, Stat5b, and Jak2 were immunoprecipitated from whole-cell lysates with anti-Stat5a, anti-Stat5b (4 μL/mL; Millipore), or anti-Jak2 (Millipore) pAbs. For immunoblotting, primary antibodies were used at the following concentrations: anti-phosphotyrosine-Stat5a/b (Y694/Y699) mAb

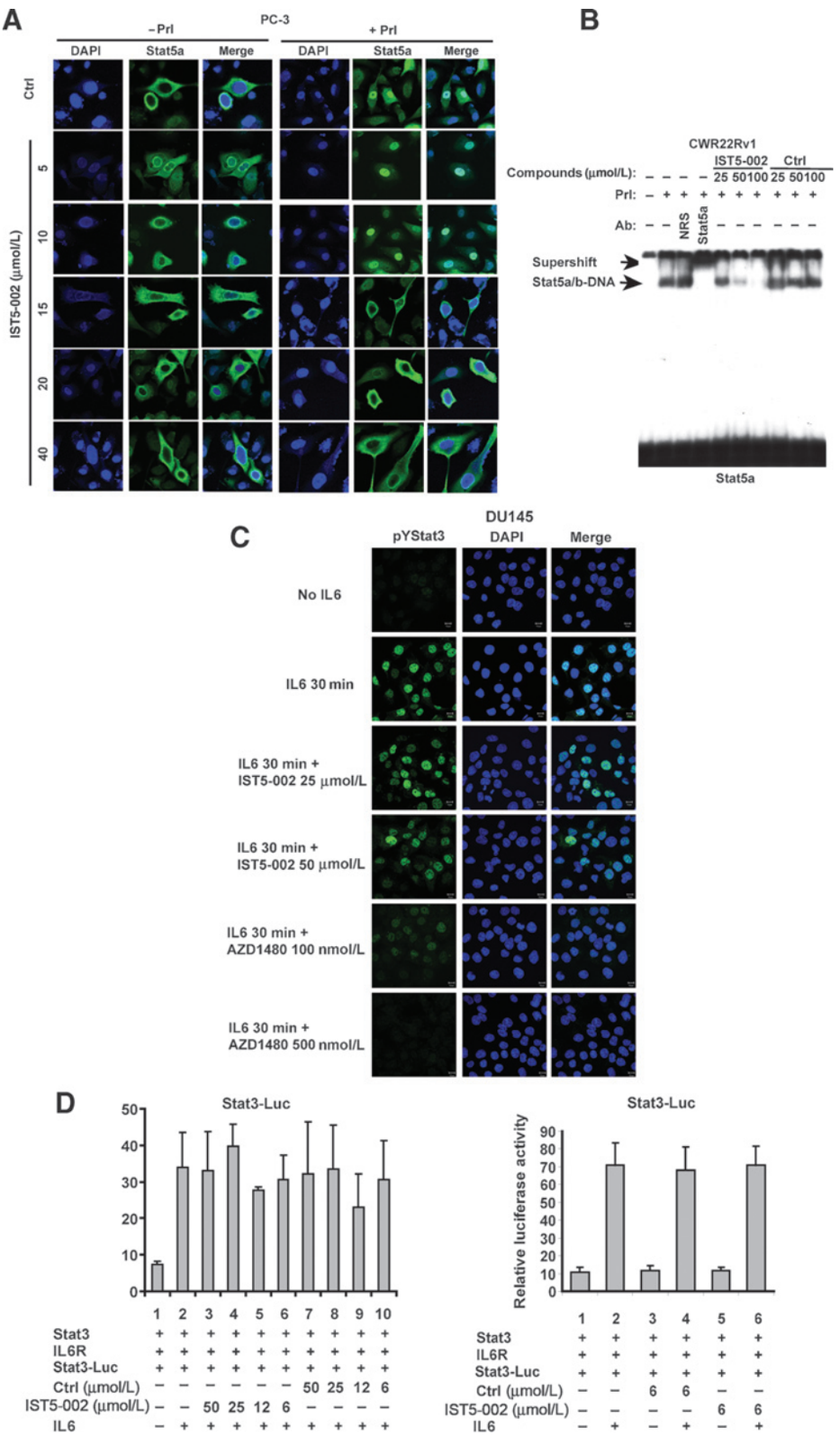

Figure 2.
IST5-002 inhibits Stat5 nuclear translocation and DNA binding of Stat5 target genes. A, IST5-002 inhibits Prl-induced nuclear translocation of Stat5 in prostate cancer cells. PC-3 cells were infected with adenoviruses expressing wild-type Stat5a (AdWTStat5a; MOI = 4) and human Prl-receptor (AdPrlR; MOI = 4). Serum-starved (16 hours) cells were treated with IST5-002 or Ctrl (2 hours), followed by stimulation with 10 nmol/L hPrl (30 minutes). Immunostaining of Stat5 is demonstrated by indirect immunofluoresence (green), while DAPI staining (blue) shows the nuclei. B, IST5-002 inhibits binding of Stat5 to DNA shown by EMSA analysis using the Stat5-response element of β-casein gene as the probe. COS-7 cells were transiently cotransfected with pStat5a and pPrlR, serum starved (10 hours), and treated with IST5-002 or Ctrl at indicated concentrations (2 hours) followed by stimulation with 10 nmol/L hPrl (30 minutes). The specificity of the Stat5–DNA binding complex was demonstrated by supershift with anti-Stat5a pAb versus normal rabbit serum (NRS). C, IST5-002 does not inhibit nuclear translocation of Stat3 in prostate cancer cells. Serum-starved DU145 cells were pretreated with IST5-002, AZD1480, or vehicle (2 hours) before stimulation with 5 nmol/L IL6 (30 minutes). Immunostaining of Stat3 is demonstrated by indirect immunofluoresence (green), while DAPI staining (blue) shows the nuclei. D, IST5-002 does not inhibit transcriptional activity of Stat3 in prostate cancer cells. LNCaP cells were transiently cotransfected with pStat3, pIL6-receptor (pIL6R), pStat3-Luc, and pRL-TK (*Renilla* luciferase). Cells were serum-starved (10 hours), pretreated with 6.0 μmol/L IST5-002, or Ctrl (2 hours), followed by stimulation with 50 ng/mL IL6 (16 hours). Relative luciferase activities were determined, and mean values of three independent experiments performed in triplicate ± SE values are indicated by bars.

(1 μg/mL; Advantex BioReagents), anti-Stat5ab mAb (1:250; BD Biosciences), anti-c-Abl mAb (1:500; Calbiochem), anti-Grb2 mAb (5:100; BD Biosciences), anti-β-actin pAb (1:4,000; Sigma), anti-cyclin D1 mAb (1:1,000; BD Biosciences), anti-pPAK1/2 (1:1,000; Cell Signaling Technology), anti-Bcl-xL pAb (1:1,000; Cell Signaling Technology), and anti-phosphotyrosine mAb (1:1,000; Millipore).

Cell-based immunoassay for tyrosine-phosphorylated Stat5a/b

T47D cells in 96-well plates were serum-starved for 16 hours, pretreated with IST-002 at the indicated concentrations for 2 hours, followed by stimulation with hPrl (2 nmol/L) for 15 minutes, and fixation in 20°C acetone/methanol followed by incubation with anti-pStat5a/b rabbit mAb (1:200; Cell Signaling Technology) and secondary horseradish peroxidase (HRP)–conjugated anti-rabbit Ab (1:2,000; Cell Signaling Technology). The amount of phospho-Stat5a/b was evaluated using 1-Step Ultra TMB substrate (Thermo Scientific) at 450 nm. Cells cultured in the absence of IST-002 and treated with or without prolactin served as positive and negative controls, respectively. The inhibition curve and IC_{50} were derived from triplicate measurements using SigmaPlot.

Kinase activity assay

Inhibitory activity of IST5-002 was tested against a panel of 50 kinases using KinaseSeeker Technology (Luceome Biotechnologies). Prior to initiating the kinase profiling, IST5-002 was evaluated for false positive activity against split-luciferase. For the kinase assays, each Cfluc-Kinase was translated along with Fos-Nfluc using a cell-free system (rabbit reticulocyte lysate) at 30°C for 90 minutes. An aliquot (24 μL) of this lysate containing either 1 μL of DMSO (for no-inhibitor control) or compound solution in DMSO (1 μmol/L final concentration) was incubated for 30 minutes at room temperature followed by 1 hour in the presence of a kinase-specific probe. Eighty microliters of luciferin assay reagent was added to each solution and luminescence was immediately measure in a luminometer. Profiling data for all kinases were plotted as % activity remaining versus kinases profiled.

Determination of Stat5a dimerization by coimmunoprecipitation

The dimer formation of Stat5a was analyzed as described previously (4) and in the Supplementary Methods. Cells were serum-starved for 16 hours, followed by pretreatment with IST5-002 or the control compound (Ctrl) for 2 hours at indicated concentrations, and stimulated with hPrl (10 nmol/L) in serum-free medium for 30 minutes. Whole-cell lysates were immunoprecipitated with anti-Myc mAb (2 μg/sample; Santa Cruz Biotechnology) and immunoblotted with anti-Flag mAb (1:1,000; Genomics), anti-Myc mAb (1:1,000; Santa Cruz Biotechnology), and anti-actin pAb (1:4,000; Sigma-Aldrich).

Generation of adenoviral vectors for gene delivery of Stat5 and PrlR

pcDNA-CMV-WT-*STAT5A* and pcDNA-CMV-constitutively active *STAT5A* (CAStat5a; Stat5aS710F; ref. 38) were cloned to adenoviral vector using BD Adeno-X Expression System 2 (BD Biosciences Clontech). pcDNA-CMV-WT-*STAT5A* and pcDNA-CMV-constitutively active *STAT5A* (CAStat5a; Stat5aS710F; ref. 5) were cloned to adenoviral vector using BD Adeno-X Expression System 2 (BD Biosciences Clontech) according to the manufacturer's protocol. The purified recombinant adenovirus was linearized by *Pac*I digestion and transfected to QBI-293A cells (Qbiogene) to produce infectious recombinant adenoviruses. The resulting AdWTStat5a, AdCAStat5a, and AdPrlR primary viral stocks were expanded in large-scale cultures, purified by double cesium chloride gradient centrifugation, and titrated by a standard plaque assay method in QBI-293A cells, as per the manufacturer's instructions.

Immunofluoresence cytochemistry of Stat5a/b and Stat3

PC-3 cells were infected with AdWTStat5a and AdPrlR at MOI 4. Serum-starved (10 hours) cells were pretreated with IST5-002 or control compound (2 hours) and stimulated with 10 nmol/L Prl (30 minutes). For analysis of IST5-002 efficacy in inhibition of Stat3 nuclear translocation, DU145 cells were serum-starved, pretreated with IST5-002, AZD1480 or vehicle at indicated concentrations for 2 hours, before cells were stimulated with IL6 (ProSpec-Tany Technogene) at 5 nmol/L (30 minutes). Fixed cells were incubated with rabbit anti-Stat5 pAb (1:200; Santa Cruz Biotechnology) or anti-pYStat3 pAb (1:100; Cell Signaling Technology), followed by goat anti-rabbit fluorescein IgG (1:200; Vector Laboratories), as described previously (23).

Electrophoretic mobility shift assay

Electrophoretic mobility shift assays (EMSA) were conducted as we have described previously (23).

Cell viability and DNA fragmentation assay

Cell viability was determined by the CellTiter 96 Aqueous Assay Kit (Promega). The number of living cells was also determined by counting the attached versus nonattached cells using a hemacytometer and Trypan blue exclusion. DNA fragmentation was analyzed by photometric enzyme immunoassay according to the manufacturer's instructions (Cell Death Detection ELISA^{PLUS}; Roche).

Caspase-3 activation assay

CWR22Rv1 cells were treated with IST5-002 (12.5 μmol/L) or vehicle for indicated periods of time. Caspase-3 was captured by anti-caspase-3 mAb, followed by caspase-3–mediated enzymatic cleavage of 7-amino-4-trifluoromethyl-coumarin (AFC) substrate measured at 505 nm. In Stat5a/b rescue experiments, CAStat5a was expressed using an adenoviral vector (MOI = 2) 6 hours prior to treatment of cells with IST5-002 (12.5 μmol/L) or vehicle for 72 hours.

Cell-cycle analysis

Cells were treated with IST5-002, vehicle, or control compound for 24, 48, and 72 hours, fixed and stained with propidium iodide (PI) and RNase A (Sigma-Aldrich). PI fluorescence intensity was analyzed by a flow cytometer using FL-2 channel.

Colony formation assay

CML-blast crisis lines and CML $CD34^+$ primary cells were plated in the presence of DMSO, 5 μmol/L IST-002, or 5 μmol/L control compound. After 3 hours of incubation, 1×10^3(K562), 2.5×10^3 (BV173 and KCL22), or 3×10^4 (CML) cells were plated in duplicate in methylcellulose and the number of colonies was assessed 5 to 10 days after plating.

RNA expression profiling

RNA from vehicle, IST5-002, scramble shRNA, and Stat5a/b-shRNA was profiled in triplicate using the Affymetrix

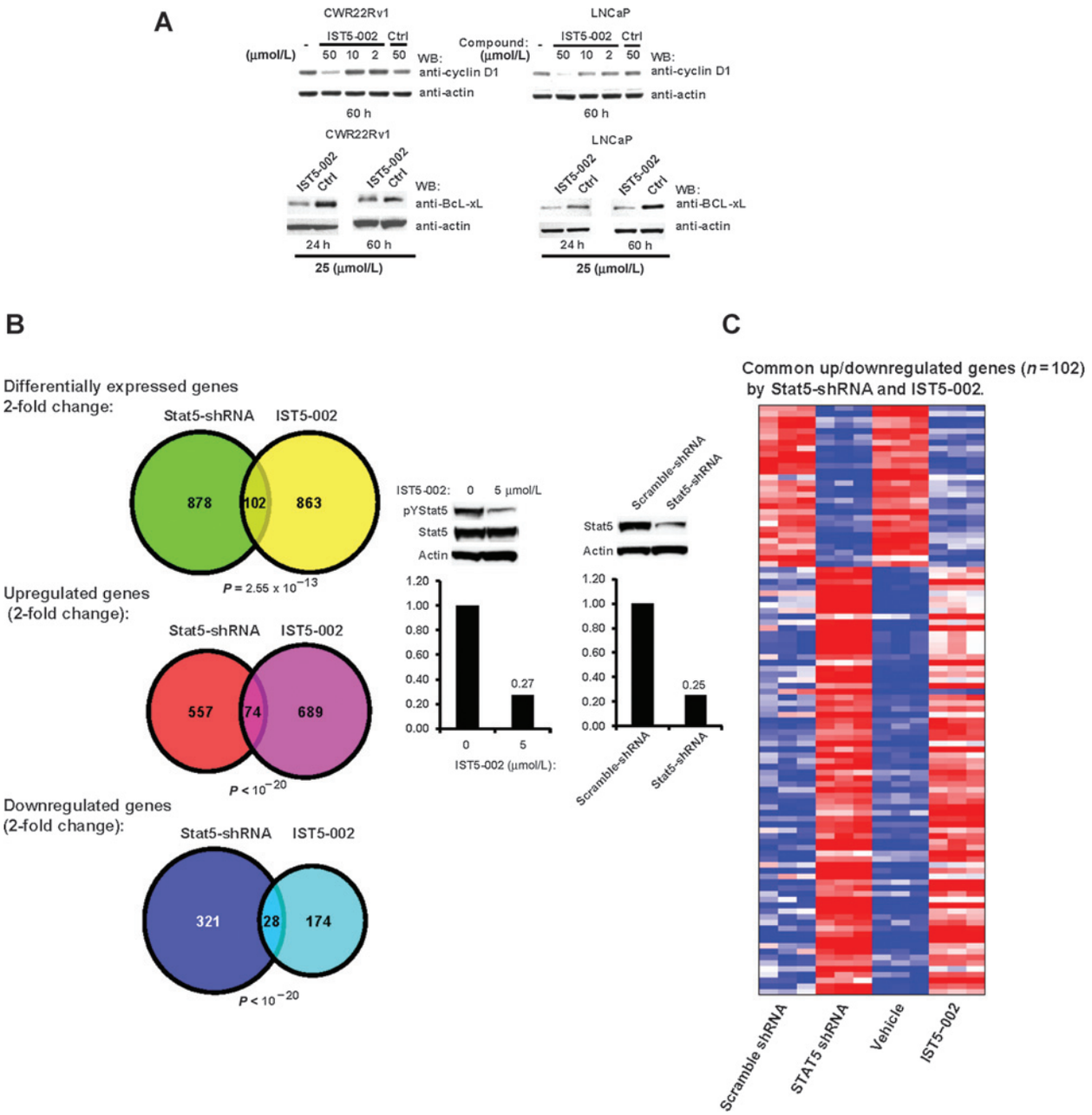

Figure 3.
IST5-002 inhibits expression of Stat5 target genes. A, IST5-002 downregulates the expression of Stat5 target genes cyclin D1 and Bcl-xL in prostate cancer cells. Exponentially growing CWR22Rv1 and LNCaP cells were treated with IST5-002 or Ctrl and whole-cell lysates were immunoblotted with anti-cyclinD1 mAb or anti-Bcl-xL pAb. B, expression profiling of genes regulated by both genetic knockdown of Stat5 and IST5-002 in CML cells. Stat5 was suppressed in K562 cells by lentiviral expression of Stat5 shRNA versus scramble control for 6 days or by treatment of the cells with IST5-002 (5 μmol/L) for 48 hours. Venn diagrams of Stat5–shRNA and/or IST5-002–regulated genes in K562 cells meeting criteria for significant up/downregulation (FDR-adjusted $P < 0.05$, >2-fold change; left). Inhibition of Stat5 protein expression and phosphorylation demonstrated by immunoblotting of whole-cell lysates with anti-pYStat5 mAb and anti-Stat5 mAb versus anti-actin pAb as loading control (right). C, the heatmap represents patterns of differential expression for 102 genes (listed in Supplementary Table S2) significantly regulated by both Stat5 knockdown and IST5-002. Red, higher expression; blue, lower expression.

GeneChip Human Gene 1.0 ST microarray platform. Differential gene expression comparisons were performed for IST5-002 versus vehicle, and Stat5a/b-shRNA versus scramble-shRNA using a *t* test with false discovery rate correction. Protocols for RNA preparation, hybridization, scanning, and statistical analysis are described in detail in the Supplementary Methods. The accession number for the sDNA array data are GSE61312.

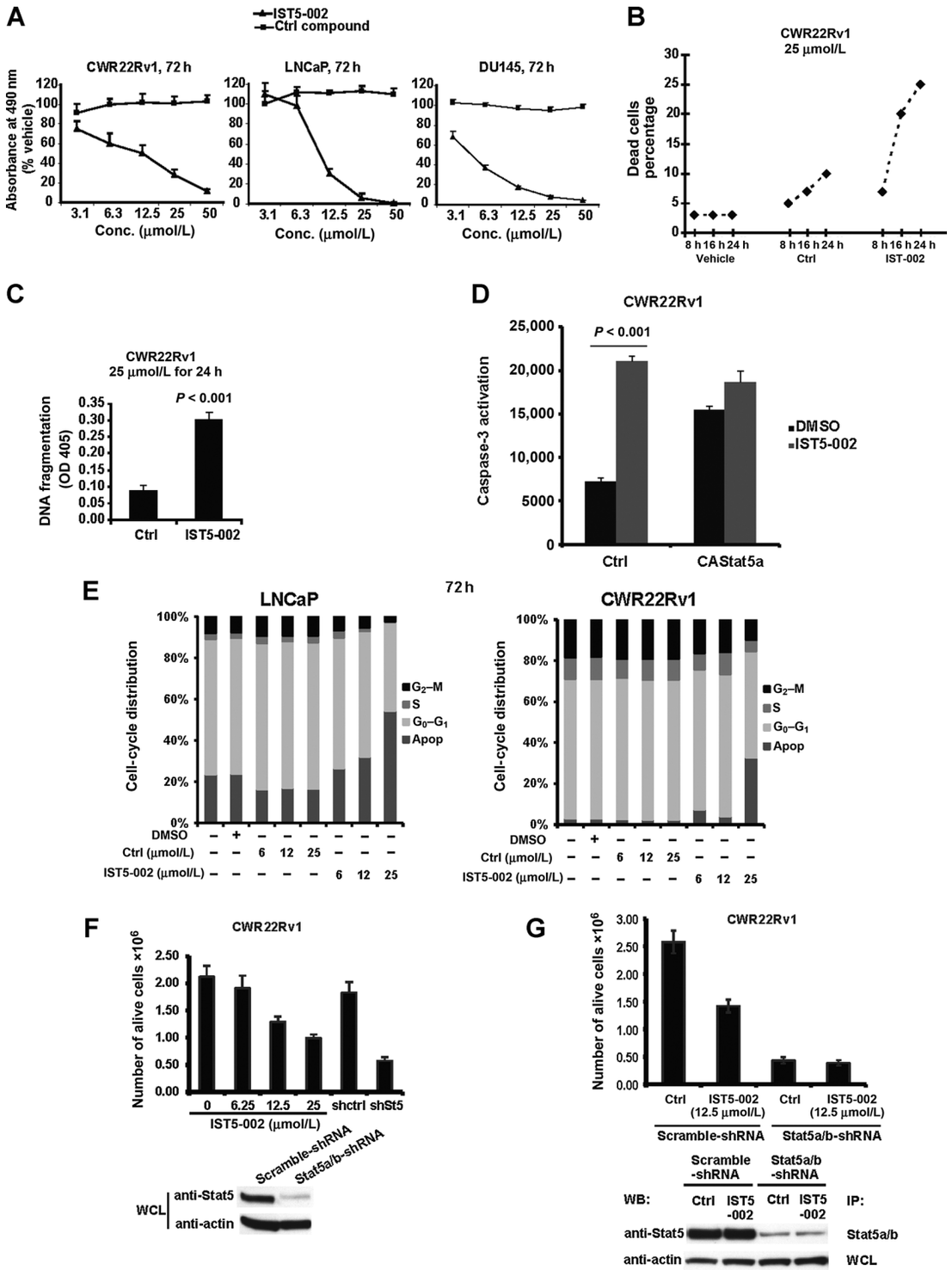

Figure 4.

IST5-002 decreases viability of human prostate cancer cells *in vitro*. A, CWR22Rv1, LNCaP, and DU145 cells were treated with IST5-002, Ctrl, or vehicle, and the fraction of living cells was determined by MTS (3-(4,5-dimethylthiazolyl-2)-2,5-diphenyl-tetrazolium bromide) metabolic activity assay. B, CWR22Rv1 cells were treated with 25 μmol/L IST5-002, Ctrl, or vehicle (24 hours) followed by Trypan blue exclusion and dead cells were manually counted. C, in parallel wells, nucleosomal DNA fragmentation, indicating cell death due to apoptosis, was demonstrated by nucleosomal ELISA at 405 nm. D, IST5-002 induces an increase in caspase-3 activation in CWR22Rv1 cells (72 hours; $P < 0.001$), which was counteracted by expression of constitutively active (CA) Stat5a/b. CWR22Rv1 cells were infected with adenovirus expressing CAStat5a (AdCAStat5a; MOI = 2) 12 hours prior to treatment of cells with IST5-002 (12 μmol/L) or vehicle, followed by determination of caspase-3 activation by fluorometric immunosorbent enzyme assay. (*Continued on the following page.*)

Human prostate cancer xenograft tumor growth studies

Castrated male athymic nude mice were purchased from Taconic and cared for according to the institutional guidelines. Mice were implanted with sustained-release DHT pellets (60-day release, 1 pellet/mouse; Innovative Research of America) 3 days before prostate cancer cell inoculation. Briefly, 1.5×10^7 CWR22Rv1 cells were mixed with 0.2 mL of Matrigel (BD Biosciences), and inoculated subcutaneously (s.c.) into flanks of nude mice (one tumor/mouse) as described previously (2–4). After 1 week, tumor sizes were measured, and mice were randomly distributed into five groups (10 mice/group). Mice were treated daily for 10 days by intraperitoneal (i.p.) injections with 0.2 mL of IST5-002 dissolved in 0.3% hydroxypropyl cellulose (HPC; Sigma-Aldrich) at 25, 50, or 100 mg/kg body weight, or with 0.2 mL 0.3% HPC solution, or no treatment, and tumor sizes were measured three times per week. Tumor volumes were calculated using the following formula: 3.14 × length × width × depth/6. When the tumors reached 15 to 20 mm in diameter in the control groups, mice were sacrificed and tumor tissues were harvested. Percentage changes in tumor volume of each group are presented.

***Ex vivo* organ culture testing of Stat5-inhibitor efficacy in clinical prostate cancers**

Prostate cancer specimens were obtained from patients with localized or locally advanced prostate cancer undergoing radical prostatectomy and bilateral iliac lymphadenectomy (Table 1). The Thomas Jefferson University Institutional Review Board approved this work to be in compliance with federal regulations governing research on deidentified specimens [45 CFR 46.102(f)]. A zero-sample prior to organ culture of each individual prostate cancer was formalin-fixed for the analysis of nuclear Stat5a/b status. Prostate organ cultures were performed as described earlier (4, 7, 34, 39) and in the Supplementary Methods.

Stat5a/b immunohistochemistry and TUNEL assay of paraffin-embedded tissue sections

Immunohistochemistry (IHC) staining of Stat5a/b and terminal deoxynucleotidyl transferase–mediated dUTP nick end labeling (TUNEL) assay were performed as described previously (1, 3–5, 7, 8, 21). Viable, active nuclear Stat5a/b-positive, Stat3-positive, or apoptotic (fragmented DNA) cells versus total number of cells (viable and dead) were counted for 3 views/tumor and 1 view covering each organ culture explant (20–25 explants per treatment group per patient) and expressed as percentages, as demonstrated previously (4). The average cell number per explant is determined of a sample of each patient prior to culture. All percentages within each treatment group (tumor or organ culture explant) were averaged.

Statistical analyses

Mixed-effects linear regression was used to model log 10–transformed tumor volumes. A quadratic curve in time was modeled separately for each treatment group. Random terms were included for the intercept, slope, and quadratic effect, allowing for each animal's curve to differ from the mean curve in its group. Differences in the groups with respect to the geometric mean tumor volume at days 1, 3, 6, 8, and 10 were tested, and at day 10, pairwise comparisons were performed to identify which groups differed from each other. P values were adjusted using Bonferroni method. $P < 0.05$ was considered significant.

For tumor cell viability and nuclear Stat5 or Stat3 levels, analysis of variance implemented in SAS ProcMIXED was used to test for differences in responses across groups. Pairwise comparisons were performed to compare each inhibitor dose to the control groups and P values for pairwise comparisons were adjusted using the Bonferroni method.

For cancer cell viability and nuclear Stat5 content in organ explant cultures, mixed-effects linear regression was used for statistical analysis of responders, followed by pairwise comparisons adjusted using the Bonferroni method. For nonresponders, the Kruskal–Wallis test was used because of the small number of measurements for each group.

Results

Virtual screen identifies a small molecule inhibitor of Stat5a/b phosphorylation and dimerization

To identify a family of Stat5a/b inhibitor compounds, we used *in silico* structure-based screening and medicinal chemistry. Docking of the most promising compound, inhibitor of Stat5-002 (IST5-002), to the binding site of the Stat5b SH2 domain is depicted (Fig. 1A–C). Chemical structures of IST5-002 (MW 437 Da), a randomly selected control compound (Ctrl) of similar molecular weight (343 Da; Fig. 1D) and other IST5-family members (Supplementary Fig. S1) are shown.

To determine whether IST5-002 blocks Stat5a/b transcriptional activity, PC-3 cells were cotransfected with PrlR, Stat5a or Stat5b, and a Stat5a/b-luciferase reporter (β-casein-luciferase). Cells were treated with IST5-002 or Ctrl for 2 hours prior to and during Stat5a/b activation by stimulation with human prolactin (hPrl, 10 nmol/L; 16 hours). IST5-002 robustly inhibited transcriptional activity of Stat5a ($IC_{50} = 1.5$ μmol/L) and Stat5b ($IC_{50} = 3.5$ μmol/L) in a dose-dependent manner, compared with Ctrl (Fig. 1E). Design and synthesis of IST5-002 analogs and structure–activity relationship (SAR) studies (Supplementary Table S1) identified a family of IST5-002 inhibitors (Supplementary Fig. S1) that displayed efficacies comparable with IST5-002.

To analyze whether IST5-002 suppresses formation of transcriptionally active phosphorylated dimers, Bcr-Abl–positive K562 cells were treated with increasing concentrations of IST5-002 (3 hours), using pimozide (15) and Ctrl as positive and negative controls, respectively. Remarkably, IST5-002 blocked Bcr-Abl–induced Stat5a/b phosphorylation at 5 μmol/L (Fig. 1F). At the same time, pimozide, a previously reported Stat5a/b inhibitor

(*Continued.*) E, IST5-002 increases the fraction of dead prostate cancer cells in cell-cycle analysis. LNCaP and CWR22Rv1 cells were treated with IST5-002 or Ctrl for 72 hours at indicated concentrations followed by FACS analysis. F, CWR22Rv1 cells were treated with IST5-002 at indicated concentrations or transduced with lentiviral shStat5a/b (Stat5a/b–shRNA) or control shRNA (scramble-shRNA) for 72 hours and alive cells were counted manually after Trypan blue exclusion. G, to test the effect of IST5-002 on prostate cancer cell viability after genetic knockdown of Stat5a/b, CWR22Rv1 cells were first transduced with lentiviral Stat5a/b shRNA (Stat5a/b-shRNA) or control shRNA (scramble-shRNA). After 24 hours, the cells were treated with IST5-002 (12.5 μmol/L) or control compound (Ctrl) for 48 hours and alive cells were counted manually after Trypan blue exclusion.

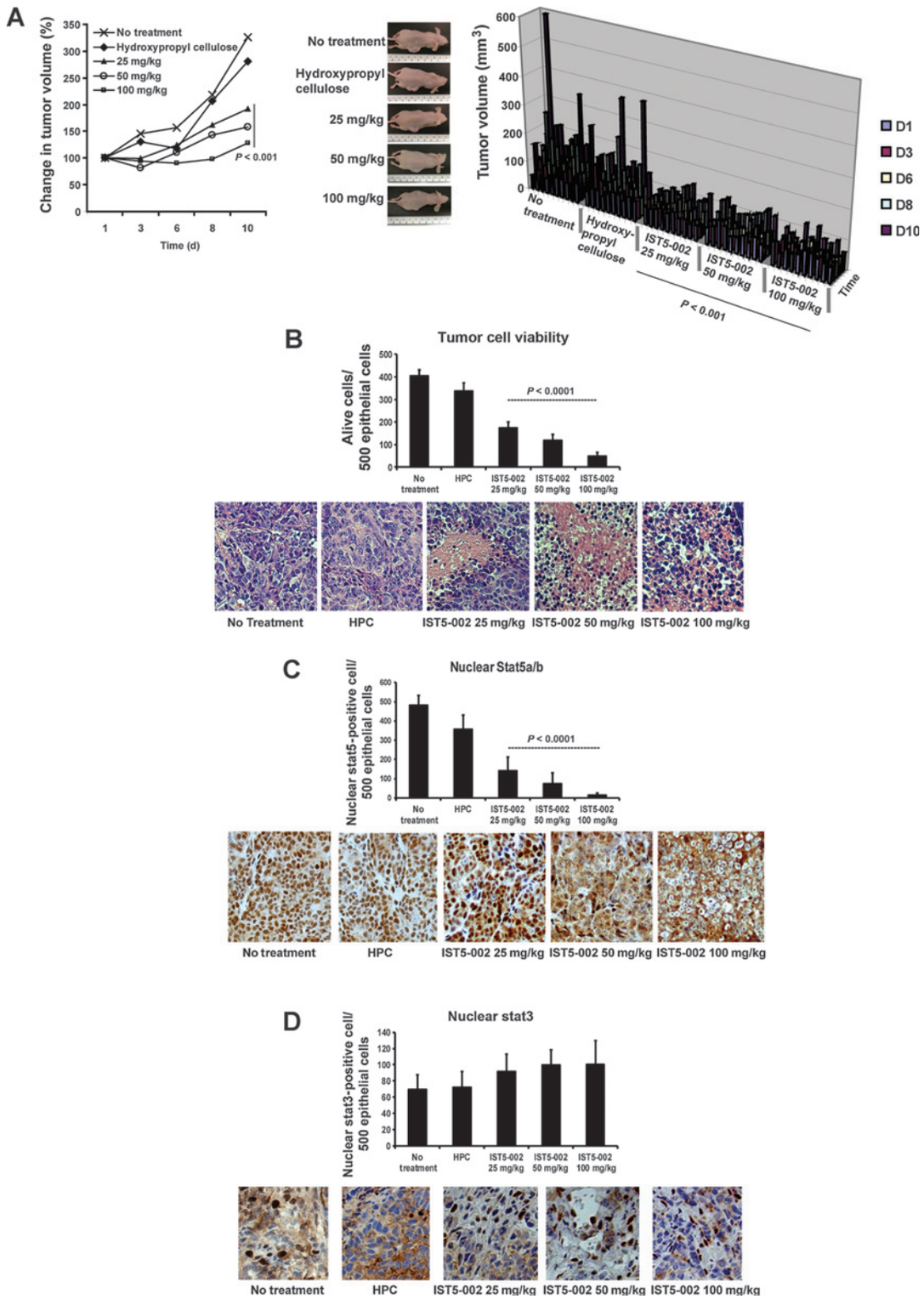

Figure 5.
IST5-002 inhibits prostate cancer xenograft tumor growth *in vivo* in nude mice. A, CWR22Rv1 prostate cancer cells were inoculated subcutaneously into the flanks of castrated athymic nude mice supplied with sustained-release 5α-DHT pellets ($n = 10$/group, 1 tumor/mouse, 1.5×10^7 CWR22Rv1 cells per site, 1 DHT pellet/mouse). Mice were treated with IST5-002 (25, 50, and 100 mg/kg) or vehicle (HPC) as control i.p. daily, with a group with no treatment as an additional control. Tumor sizes were measured every 3 days, and tumor volumes were calculated using the formula $V = (\pi/6) \times d_1 \times (d_2)^2$, with d_1 and d_2 being two perpendicular tumor diameters. (*Continued on the following page.*)

(15), required 20 to 40 μmol/L to fully block Stat5a/b phosphorylation under these same conditions. However, pimozide is likely to induce a number of off-target effects related to the high concentrations needed for Stat5a/b inhibition. IST5-002 did not affect Bcr-Abl tyrosine phosphorylation levels in K562 cells (Fig. 1F). Next, serum-starved CWR22Rv1, HC-11, and T47D cells were treated with IST5-002 (2 hours), followed by stimulation with hPrl (30 minutes). For CWR22Rv1 (Fig. 1G) and HC-11 (Supplementary Fig. S2A) cells, Stat5a/b were immunoprecipitated and immunoblotted with anti-pYStat5a/b antibody (Fig. 1G), while a cell-based immunoassay was used to monitor Stat5a/b phosphorylation in T47D cells (Supplementary Fig. S2B). IST5-002 blocked phosphorylation of Stat5a/b (CWR22Rv1, $IC_{50} = 22$ μmol/L; HC-11, $IC_{50} = 12$ μmol/L; T47D, $IC_{50} = 24.8$ μmol/L), while total Stat5a/b levels remained unaffected. Phosphorylation of Jak2 was unaffected by IST5-002, indicating that IST5-002 does not inhibit Jak2 (Fig. 1G). Moreover, kinase activity profiling assay indicated no specific inhibition of other kinases in a panel of 50 kinases by IST5-002 (Supplementary Fig. S3), including activity of PAK1/2 (Supplementary Fig. S4; ref. 40). To test whether IST5-002 disrupts dimerization of Stat5a/b, we generated and cotransfected *FLAG*- and *MYC*-tagged Stat5a into PC-3 cells along with PrlR. Serum-starved cells were treated with IST5-002 or Ctrl before stimulation with hPrl (10 nmol/L; 30 minutes). Lysates were immunoprecipitated with anti-Myc antibodies and immunoblotted with anti-Flag or anti-Myc antibodies. As expected, hPrl stimulation induced Stat5a dimerization, which was inhibited by IST5-002 ($IC_{50} = 11$ μmol/L; Fig. 1H). We conclude that IST5-002 effectively blocks molecular events associated with Stat5a/b activation, including phosphorylation, dimerization, and transcriptional activity.

IST5-002 suppresses downstream signaling events and target gene expression induced by Stat5a/b in prostate cancer and CML cells

We next investigated whether IST5-002 disrupts downstream signaling events induced by Stat5a/b activation. To assess if nuclear translocation of Stat5a/b is affected, we expressed Stat5a and PrlR in PC-3 cells and treated serum-starved cells with IST5-002 (2 hours), prior to stimulation with hPrl (10 nmol/L; 30 minutes). In the absence of hPrl, Stat5a was predominantly localized in the cytoplasm, as demonstrated by immunocytochemistry (Fig. 2A). Addition of hPrl robustly induced Stat5a nuclear translocation, which was abrogated by IST5-002 at 15 μmol/L (Fig. 2A).

To determine whether IST5-002 inhibits DNA binding of activated Stat5a/b, we used EMSA using the Stat5a/b response element of the β-casein gene promoter as a probe (Fig. 2B). COS-7 cells transfected with PrlR and Stat5a were serum-starved and pretreated with IST5-002 (2 hours), followed by hPrl stimulation (10 nmol/L; 30 minutes). As predicted, IST5-002 reduced binding of Stat5a/b to its DNA target sequence by approximately 50% at 25 μmol/L, compared with Ctrl-treated cells (Fig. 2B).

To evaluate specificity of IST5-002 for Stat5a/b, we tested the ability of IST5-002 to inhibit nuclear translocation and transcriptional activity of IL6-induced Stat3. Serum-starved DU145 cells were pretreated with IST5-002 or a positive control compound, Jak2 inhibitor AZD1480 (4, 41), before stimulation with IL6 (5 nmol/L). Although AZD1480 effectively suppressed Stat3 nuclear translocation, IST5-002 had no demonstrable effect, even at a higher concentration (50 μmol/L; Fig. 2C). We reconstituted the IL6-receptor–Stat3 signaling pathway in LNCaP cells and introduced a Stat3-luciferase reporter. Serum-starved cells were pretreated with IST5-002 (1 hour) and stimulated with IL6 (50 ng/mL; 16 hours). IST5-002 failed to block transcriptional activity of Stat3 (Fig. 2D) at a concentration that was highly effective at inhibiting Stat5a/b-driven transcription (Fig. 1E).

To assess the ability of IST5-002 to regulate the expression of Stat5a/b target genes in prostate cancer cells, CWR22Rv1 and LNCaP cells were treated with increasing concentrations of IST5-002 or Ctrl (48 hours; Fig. 3A), or a single dose of IST5-002 (25 μmol/L) or Ctrl for the indicated times (Supplementary Fig. S5A). Immunoblotting of prostate cancer cell lysates showed that IST5-002 reduced expression of both Bcl-xL and cyclin D1 (Fig. 3A and Supplementary Fig. S5A), both previously demonstrated as Stat5a/b target genes in prostate cancer cells (2). We further assessed the gene expression profiles induced by genetic (Stat5a/b shRNA) or pharmacologic (IST5-002) knockdown of Stat5a/b in CML cells, as verified by immunoblotting (Fig. 3B). Genes (Supplementary Fig. S5B) regulated by both Stat5a/b-silencing and IST5-002 in CML cells are presented as Venn diagrams (Fig. 3B). The statistically significant ($P < 0.01$) similarity between the gene expression changes induced by IST5-002 treatment and Stat5a/b knockdown in K562 cells indicate that these transcriptional changes are primarily due to loss of Stat5a/b activity and not to off-target effects (Fig. 3C and Supplementary Tables S2–S5). Among known Stat5a/b target genes regulated by IST5-002 were cyclin D2 (−2.3-fold), Pim1 (−1.7-fold), Pim2 (−1.7-fold), Myc (−1.7-fold), SOCS3 (−1.3-fold), CISH (−2.3-fold), and TRIB2 (−1.4-fold; Supplementary Table S5). Gene ontology enrichment analysis revealed genes involved in metabolic processes, proliferation, processing of extracellular stimuli and remodeling actin cytoskeleton (Supplementary Fig. S5C).

IST5-002 suppresses Stat5a/b-mediated growth of prostate cancer through induction of apoptosis in experimental models of prostate cancer *in vitro*, *in vivo*, and *ex vivo*

To investigate the effect of IST5-002 in prostate cancer cell growth, we treated three human prostate cancer cell lines with IST5-002 or Ctrl (72 hours). In all three cell lines, IST5-002 decreased viable cells by 50% to 80% at 12.5 μmol/L ($P < 0.001$; Fig. 4A). Treatment of CWR22Rv1 cells with 25 μmol/L IST5-002 (24 hours) resulted in a 5-fold increase in dead cells, as detected by Trypan blue exclusion (Fig. 4B). In parallel wells, IST5-002 increased nucleosomal DNA fragmentation by 230%, suggesting that the mode of cell death was apoptotic

(*Continued.*) Columns represent percentage change in tumor volume and growth of individual tumors. Tumor growth was significantly ($P < 0.001$) suppressed in all IST5-002 treatment groups compared with the control groups. B, IST5-002 induces apoptotic cell death in CWR22Rv1 prostate cancer xenograft tumors. Hematoxylin and eosin staining of the sections demonstrates loss of viable tumor cells and accumulation of dead cells (arrows) in IST5-002–treated CWR22Rv1 xenograft tumors versus controls. C, immunostaining of nuclear active Stat5a/b or (d) Stat3 of paraffin-embedded sections of the prostate xenograft tumors.

($P < 0.001$; Fig. 4C). IST5-002 (12.5 μmol/L) induced a 3-fold increase in caspase-3 activation ($P < 0.001$; Fig. 4D). Importantly, overexpression of constitutively active Stat5a/b (3) by adenoviral vector (CAStat5a) 12 hours prior to treatment with 12.5 μmol/L IST5-002 prevented caspase-3 activation by IST5-002 (Fig. 4D). Cell-cycle analysis of IST5-002- or Ctrl-treated (72 hours) LNCaP and CWR22Rv1 cells revealed that IST5-002 increased the fraction of dead cells (sub-G_1) and decreased the fraction of living cells (G_2–M; Fig. 4E). Treatment of CWR22Rv1 cells for 72 hours with IST5-002 shows comparable efficacy to genetic knockdown of Stat5a/b by lentiviral transduction of Stat5a/b shRNA (Fig. 4F). Moreover, to test the effect of IST5-002 on the viability of prostate cancer cells after Stat5a/b had been genetically deleted, CWR22Rv1 cells were first transduced by lentiviral Stat5a/b shRNA versus control shRNA for 24 hours followed by treatment with IST5-002 for 48 hours. Although IST5-002 (12.5 μmol/L) induced 40% decrease in the number of viable prostate cancer cells expressing control shRNA, IST5-002 did not further affect viability of CWR22Rv1 cells depleted of Stat5a/b (shStat5a/b; Fig. 4g). IST5-002 effects were prostate cancer–specific, as viability of malignant or immortalized cell lines originating from other tissues, including lung (A549), pancreas (CAPAN), breast (T47D), fibrosarcoma (HT1080), liver (HepG2), or monkey fibroblasts (COS-7), was not affected (Supplementary Fig. S6A). When tested side-by-side, IST5-002 suppressed viability of prostate cancer (CWR22Rv1) and CML (K562) cells that both have high Stat5a/b activation, while IST5-002 did not affect viability of cell lines with low or no Stat5a/b activation (RC170N—normal prostate epithelial cell line; HT1080—fibrosarcoma cells; Supplementary Fig. S6B).

To determine whether IST5-002 efficacy extended to an *in vivo* model of prostate cancer, we inoculated CWR22Rv1 cells subcutaneously into the flanks of nude mice (Fig. 5A). Once prostate cancer xenograft tumors were established, mice were treated daily by i.p. injection of IST5-002 (25, 50, or 100 mg/kg) or vehicle (HPC). Tumor growth was significantly ($P < 0.001$) suppressed in all IST5-002 treatment groups compared with the control groups (Fig. 5A and Supplementary Fig. S7). IST5-002 induced massive loss of viable tumor cells and accumulation of dead rounded cells ($P < 0.001$; IST5-002 groups versus vehicle; Fig. 5B). IST5-002 induced cell death through apoptosis, as shown by the presence of fragmented DNA in tumor sections (Supplementary Fig. S8A). IST5-002 decreased nuclear Stat5a/b content by 60%, 78%, and 90% in groups treated with 25, 50, and 100 mg/kg, respectively, compared with vehicle (HPC; $P < 0.0001$; Fig. 5C). Intratumor levels of nuclear Stat3 were not altered at any of the doses tested (Fig. 5D). Together, these results indicate that IST5-002 suppresses prostate cancer growth *in vitro* and *in vivo*, without general toxicity in normal prostate epithelial cells or solid tumor cells originating from other organs.

To evaluate efficacy of IST5-002 in clinical prostate cancer, we exploited an *ex vivo* organ explant culture system of patient-derived prostate cancers from radical prostatectomies that we have previously established and characterized (4, 7, 34, 39). All tested clinical prostate cancers ($n = 11$) were of Gleason score 7 (Table 1), and were cultured for 7 days in the presence of IST5-002 or Ctrl at the indicated concentrations. Eight out of 11 patient-derived prostate cancers responded to IST5-002 by extensive loss of viable epithelium, starting at 25 μmol/L ($P = 0.004$; Fig. 6A). IST5-002 induced apoptotic death of explant epithelial cells in cancer acini, compared with explants cultured with Ctrl ($P = 0.002$). Apoptosis was evidenced by accumulation of dead cells in acinar lumens (Supplementary Fig. S8B). Three out of 11 prostate cancers did not show reduced epithelial cell viability in response to IST5-002 (Fig. 6A, right). Nuclear Stat5a/b contents showed a trend of downregulation by IST5-002 in the eight responsive prostate cancers, but were lower and remained largely unaffected in the nonresponsive prostate cancers (Fig. 6B). To determine whether Stat5a/b activation status could predict IST5-002 responsiveness in organ explant culture, we analyzed nuclear Stat5a/b levels in samples prior to culture. All nonresponsive prostate cancers had low or nonexistent nuclear Stat5a/b expression, while nuclear Stat5a/b immunostaining was moderate or strong in all responsive prostate cancers (Table 1). These results indicate that IST5-002 induces death of primary prostate cancer cells with high nuclear Stat5a/b expression.

IST5-002 inhibits Stat5a/b phosphorylation and induces apoptosis of imatinib-sensitive and -resistant CML cells

To determine IST5-002 efficacy in disrupting Stat5a/b phosphorylation in Bcr-Abl-driven leukemias, parental and imatinib-resistant CML cell lines (K562, KCL22, and BV173) were cultured for 24 to 72 hours with increasing concentrations of IST5-002. IST5-002 potently inhibited Stat5a/b phosphorylation in both imatinib-sensitive and -resistant CML cells ($IC_{50} = 2.5$–7 μmol/L; Fig. 7A and B). Because Stat5a/b signaling is critical for Bcr-Abl–driven growth of CML cells, we investigated whether IST5-002 affects viability of these cells. The number of living cells was assessed by Trypan blue exclusion after treatment with IST5-002 (5 μmol/L) for increasing periods of time (Fig. 8A), or by colony formation assay (Supplementary Fig. S9). In both assays, treatment with IST5-002 blocked the growth of imatinib-sensitive and -resistant CML cells. Cell-cycle analysis of IST5-002–treated cells at 48 hours showed an increase in apoptosis and a decrease in the fraction of G_2–M or S-phase cells (Fig. 8B). Furthermore, IST5-002 decreased viability of acute lymphocytic leukemia (ALL) cell line (SUP-B15) that is driven by Bcr-Abl and has high Stat5a/b phosphorylation (Fig. 8C). At the same time, IST5-002 had only marginal or no effect on the viability of EBV-immortalized B cells that express no active Stat5a/b (Fig. 8C). To evaluate IST5-002 efficacy in primary CML samples, cells obtained from three CML-chronic phase patients ($n = 3$) were plated in methylcellulose in the presence of IST5-002 and colonies were counted after 7 days. In all three samples, IST5-002 suppressed cell growth, as indicated by the dramatic decrease in the number of viable colonies (Fig. 8D). In conclusion, IST5-002 potently inhibits Stat5a/b phosphorylation and growth of imatinib-sensitive and -resistant CML cells.

Discussion

Although a critical role of Stat5a/b in pathogenesis of prostate cancer and myeloproliferative disorders has been established (1–22, 24), only a few pharmacologic Stat5a/b inhibitors are currently available for clinical development (15, 42–44). In this work, we identified a potent lead compound Stat5a/b inhibitor, IST5-002, with high efficacy in abrogating Stat5a/b signaling in prostate cancer and CML. IST5-002 potently inhibited molecular events associated with Stat5a/b activation, reduced the expression of Stat5a/b-regulated genes and induced extensive apoptotic cell death in multiple models of prostate cancer and CML *in vitro*, *in vivo* in animal models and in patient samples.

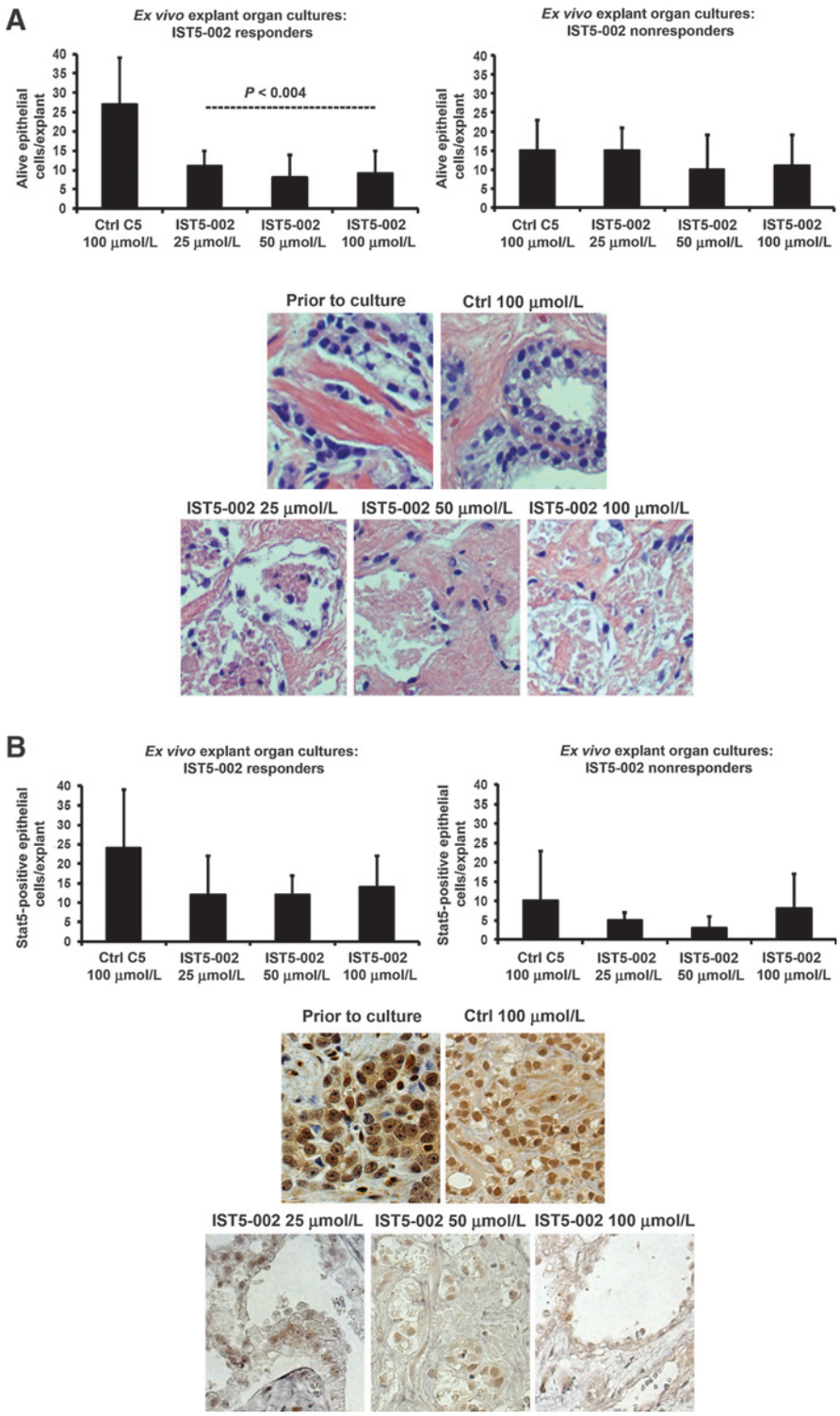

Figure 6.
IST5-002 induces death of epithelial cells in patient-derived prostate cancers *ex vivo* in organ explant cultures. A, to test responsiveness of primary prostate cancers to IST5-002, 11 localized prostate cancers (Table 1) were cultured for 7 days *ex vivo* as explant organ cultures in basal medium in the presence of IST5-002 at indicated concentrations or Ctrl. Eight prostate cancers showed loss of viable acinar epithelium in response to IST5-002 (responders, left), while in three prostate cancers, epithelial viability remained intact after IST5-002 treatment (nonresponders, right). Representative histology of an individual prostate cancer that responded to IST5-002 with extensive loss of acinar epithelium (B). Immunodetection shows intense positive immunostaining for nuclear Stat5 in explants cultured in the presence of Ctrl, while IST5-002 reduced levels of nuclear Stat5 expression. Representative immunostaining of nuclear Stat5 in a prostate cancer that responded to IST5-002 is presented.

Transcription factors are typically considered suboptimal pharmacologic targets because their function relies on protein–protein and protein–DNA interactions that are not easily disrupted by small molecules. However, our strategy was to target the SH2 domain–phosphotyrosine interaction of cytoplasmic Stat5 as a signaling molecule, prior to phosphorylation, dimerization, and nuclear translocation. Although the structure of a fragment of unphosphorylated Stat5a-SH2 domain has been determined (36), this structure lacks the phosphotyrosyl bridge and, thus, is not useful for screening molecules to target Stat5a/b SH2

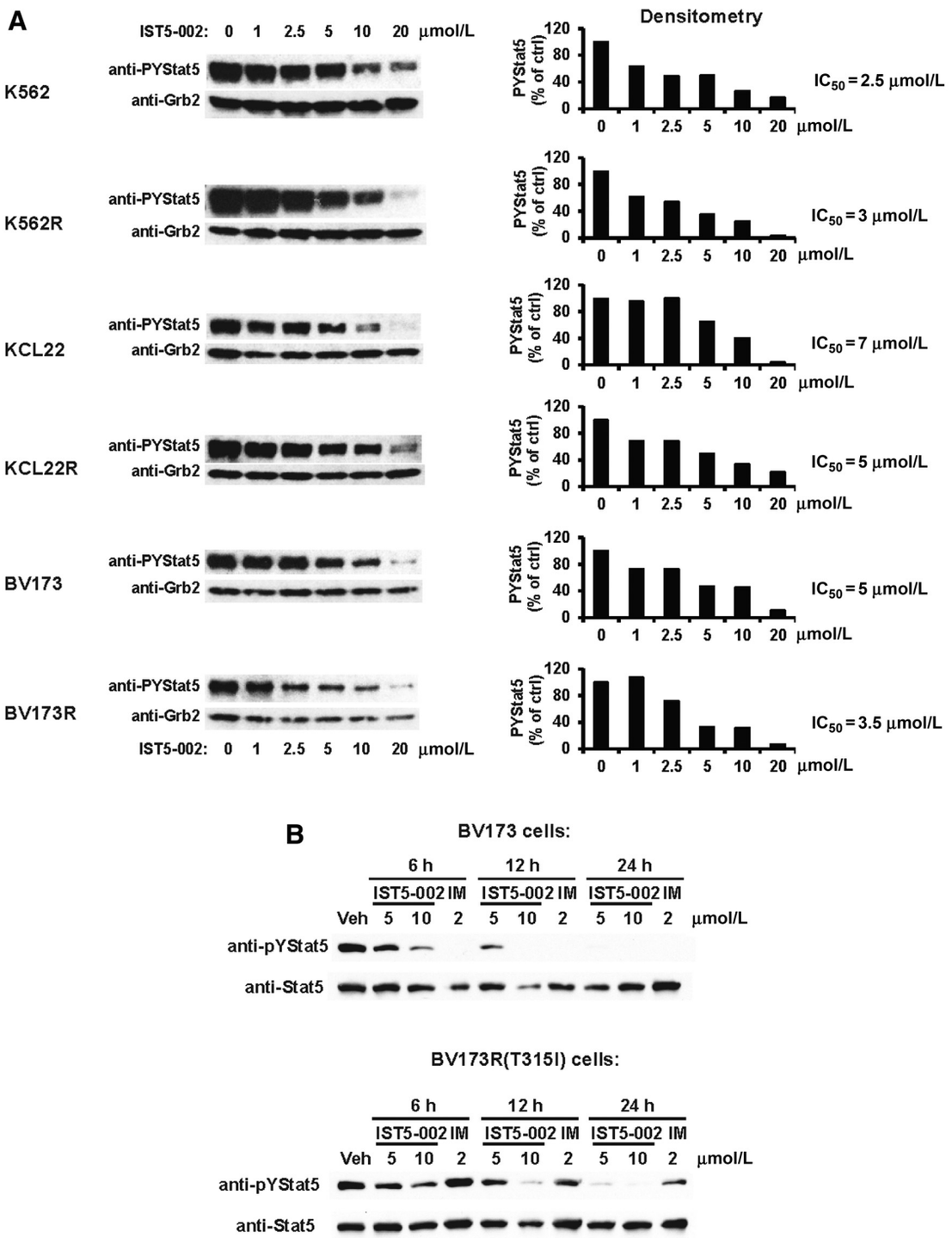

Figure 7.
IST5-002 inhibits Stat5 phosphorylation in imatinib-sensitive and -resistant CML cells. A, Western blotting (left) and densitometry (right) showing the levels of phosphorylated Stat5a/b in IST5-002–treated (12 hours) parental (sensitive) and imatinib-resistant KCL22, K562, and BV173 cells. Grb2 levels were monitored as loading control. B, Western blotting of phosphorylated Stat5a/b levels in imatinib-sensitive or -resistant (T315I) BV173 cells treated with IST5-002 or imatinib at the indicated concentrations for 6, 12, or 24 hours.

domain–pY interactions. We constructed a homology model of Stat5a/b SH2 domain based on the crystal structures of (2 hours) phosphorylated Stats (30, 37). The lead compound Stat5 inhibitor, IST5-002, showed specificity for Stat5 over Stat3. This may be due to several reasons. First, the following Stat5a/b residues were selected as binding sites for *in silico* screening: 600K,

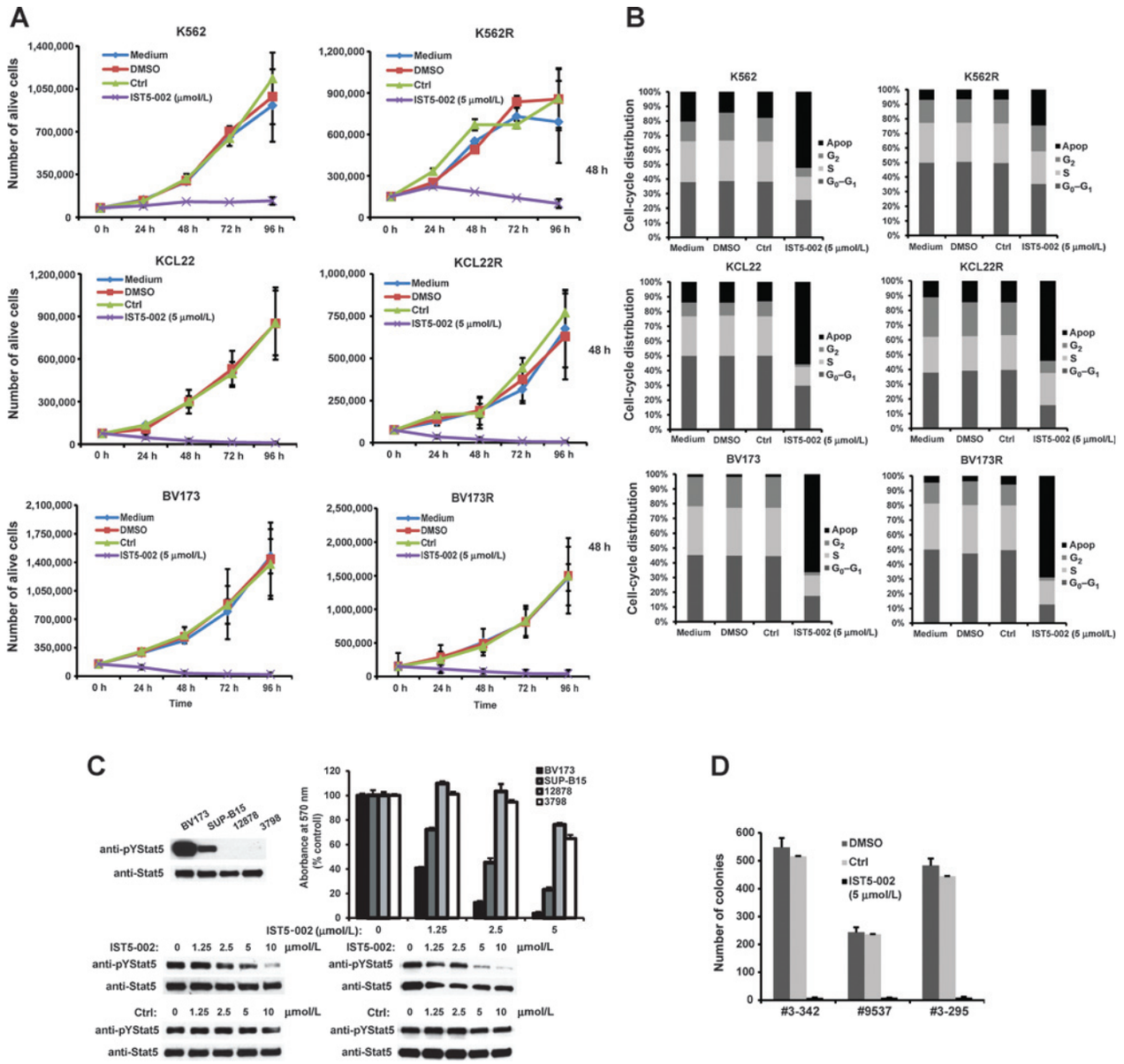

Figure 8.
IST5-002 induces extensive apoptotic death of imatinib-sensitive and -resistant CML cells. A, cell counts (Trypan blue exclusion) of IST5-002–treated (5 μmol/L) imatinib-sensitive and -resistant CML blast crisis cell lines. B, cell-cycle distribution of control (medium, DMSO, or Ctrl) or IST5-002-treated (5 μmol/L) CML-blast crisis cell lines. C, IST5-002 decreases viability of Bcr-Abl–driven lymphoid blast crisis cells (BV173) and ALL cells (SUP-B15) with high Stat5 activation, while having marginal effect on EBV-immortalized B cells with no Stat5a/b activation (12878, 3798). Levels of STAT5 phosphorylation of Bcr-Abl–expressing BV173 and SUP-B15 cell lines, and Bcr-Abl–negative, EBV-immortalized 12878 and 3798 B-cell lines (top left). Cell viability (MTT assay) of IST5-002–treated (48 hours) BV173, SUP-B15, 12878, and 3798 cell lines (top right). Levels of STAT5 phosphorylation of SUP-B15 and BV173 after 12 hours of treatment with IST5-005 or Ctrl at the indicated concentrations (bottom). D, colony formation of IST5-002–treated primary CML-chronic phase cells from patients. Colonies were counted 9 days after plating and the results are expressed as percentage colony formation inhibition of treated versus untreated cells.

604H, 618-RFSDSEIGG-626, 628T, 638-RMFWNLMPF-646, 707-VVPE-710. A comparison of these sites to the corresponding sequences in Stat3 reveals 15 differences, five of which are changes from hydrophobic (Stat5a/b) to charged (Stat3) amino acids. Moreover, the Stat3 sequence contains an inserted serine residue corresponding to a position between residues 622S and 623E in Stat5a/b. Although the data presented in the present study provide evidence for IST5-002 inhibition of Stat5a/b phosphorylation and dimerization in multiple model systems, future work will need to evaluate whether IST5-002 directly binds to the SH2 domain of Stat5a/b.

A number of nucleoside analogs structurally similar to IST5-002 (N6-benzyladenosine-5-monophosphate; ref. 45), such as 2-chlorodeoxyadenosine, fludarabine, pentostatin, and cladribine, are currently in use as anticancer drugs (46, 47). Fludarabine was recently shown to inhibit Stat1 phosphorylation and activation

but not affecting Stat5 activity (48). Analogous to fludarabine, IST5-002 inhibited molecular events involved in Stat5a/b activation while not affecting Stat3 activation. Moreover, IST5-002 induced extensive apoptosis selectively in two cancers known to be driven by Stat5a/b, prostate cancer, and CML, but was not generally cytotoxic to normal epithelial cells and affected only marginally the viability of other types of cancers not driven by Stat5a/b and with low or no Stat5a/b activation. Although IST5-002 is a close derivative of AMP, AMP or similar mononucleotides, such as GMP and cyclic AMP, had no effect on Stat5a/b activation and transcriptional activity when tested side-by-side with IST5-002 (data not shown). The IC_{50} values of IST5-002 for suppression of transcriptional activity, phosphorylation, dimerization, nuclear translocation, and viability varied between 1.5 and 22 μmol/L. This is likely due to variability in the sensitivities of different assays as well as differences between cell lines in their dependence on Stat5 for survival.

Stat5a/b has been previously established as a candidate therapeutic target protein in prostate cancer (2, 4, 9, 20, 21). IST5-002 robustly inhibited viability of Jak2-Stat5a/b–driven prostate cancer cells in culture and growth of xenograft tumors in nude mice. Moreover, IST5-002 induced extensive epithelial cell death in the majority of 11 clinical prostate cancers when tested *ex vivo* in organ explant cultures. Recently, pharmacologic targeting of Stat5a/b by a Jak2 inhibitor, AZD1480, was shown to block growth of CRPC (4). Direct pharmacologic inhibition of Stat5a/b is likely to target a larger fraction of clinical prostate cancers than targeting the kinase, because Stat5a/b is a convergence point for multiple kinases in prostate cancer, including Jak2, Src, and EGF receptor family members (3, 31–35). Of note, positive status for active Stat5a/b in 11 clinical prostate cancers predicted responsiveness to IST5-002 in *ex vivo* explant cultures, suggesting that Stat5a/b activation in prostate cancer biopsies could potentially serve as a biomarker for therapy selection.

IST5-002 induced extensive apoptotic death of both imatinib-sensitive and -resistant CML cells through potent inhibition of Stat5a/b. Moreover, IST5-002 blocked growth of primary CML-chronic phase cells. Current therapy for CML includes imatinib, dasatinib, and nilotinib, which reduce Bcr-Abl kinase activity and Stat5a/b activation (49). Our data indicated high efficacy of IST5-002, suppressing growth of both imatinib-sensitive and -resistant CML cells. However, a key concern in CML therapy is the emergence of resistance to multiple kinase inhibitors, known to develop through Bcr-Abl point mutations (particularly T315I; ref. 49) or overexpression. Pharmacologic inhibition of Stat5a/b directly may provide an improved strategy for CML therapy, either after development of resistance to current kinase inhibitors or as a part of an initial combination therapy to prevent acquired resistance.

Disclosure of Potential Conflicts of Interest

No potential conflicts of interest were disclosed.

Authors' Contributions

Conception and design: L. Gu, H. Rui, V. Njar, B. Calabretta, M.T. Nevalainen
Development of methodology: Z. Liao, L. Gu, E. Ellsworth, H. Rui, M.T. Nevalainen
Acquisition of data (provided animals, acquired and managed patients, provided facilities, etc.): Z. Liao, L. Gu, J. Vergalli, S.A. Mariani, M. De Dominici, R.K. Lokareddy, A. Dagvadorj, E. Trabulsi, C.D. Lallas, E. Ellsworth, S. Blackmon, P. Fortina, G. Xia, H. Rui, L.G. Gomella, G. Cingolani, B. Calabretta, M.T. Nevalainen
Analysis and interpretation of data (e.g., statistical analysis, biostatistics, computational analysis): Z. Liao, L. Gu, J. Vergalli, S.A. Mariani, A. Dagvadorj, A. Ertel, P. Fortina, B. Leiby, H. Rui, B. Calabretta, M.T. Nevalainen
Writing, review, and/or revision of the manuscript: Z. Liao, E. Trabulsi, S. Gupta, P. Fortina, B. Leiby, H. Rui, D.T. Hoang, L.G. Gomella, G. Cingolani, B. Calabretta, M.T. Nevalainen
Administrative, technical, or material support (i.e., reporting or organizing data, constructing databases): L. Gu, J. Vergalli, C.D. Lallas, H. Rui, D.T. Hoang, B. Calabretta, M.T. Nevalainen, P.A. McCue
Study supervision: L. Gu, V. Njar, B. Calabretta, M.T. Nevalainen
Other (design and synthesis of novel agent): P. Purushottamachar
Other (provided the compounds identified by *in silico* screening of compounds and computational aided modeling): N. Pattabiraman

Grant Support

This work was supported by grants from the NCI (2RO1CA11358-06 and 1R21CA178755-01 to M.T. Nevalainen and 1RO1CA167169-01 to B. Calabretta) and Pennsylvania Department of Health to M.T. Nevalainen, and Thomas Jefferson Univ. Intramural Funding (Dean's Support for Programmatic Research Initiatives to M.T. Nevalainen, B. Calabretta, and G. Cingolani). Shared Resources of Sidney Kimmel Cancer Center are partially supported by NIH Grant CA56036 (Cancer Center Support Grant, to Sidney Kimmel Cancer Center).

The costs of publication of this article were defrayed in part by the payment of page charges. This article must therefore be hereby marked *advertisement* in accordance with 18 U.S.C. Section 1734 solely to indicate this fact.

Received October 28, 2014; revised April 14, 2015; accepted April 15, 2015; published OnlineFirst May 29, 2015.

References

1. Ahonen TJ, Xie J, LeBaron MJ, Zhu J, Nurmi M, Alanen K, et al. Inhibition of transcription factor Stat5 induces cell death of human prostate cancer cells. J Biol Chem 2003;278:27287–92.
2. Dagvadorj A, Kirken RA, Leiby B, Karras J, Nevalainen MT. Transcription factor signal transducer and activator of transcription 5 promotes growth of human prostate cancer cells *in vivo*. Clin Cancer Res 2008; 14:1317–24.
3. Gu L, Dagvadorj A, Lutz J, Leiby B, Bonuccelli G, Lisanti MP, et al. Transcription factor Stat3 stimulates metastatic behavior of human prostate cancer cells *in vivo*, whereas Stat5b has a preferential role in the promotion of prostate cancer cell viability and tumor growth. Am J Pathol 2010;176:1959–72.
4. Gu L, Liao Z, Hoang DT, Dagvadorj A, Gupta S, Blackmon S, et al. Pharmacologic inhibition of jak2-Stat5 signaling by Jak2 inhibitor AZD1480 potently suppresses growth of both primary and castrate-resistant prostate cancer. Clin Cancer Res 2013;19:5658–74.
5. Gu L, Vogiatzi P, Puhr M, Dagvadorj A, Lutz J, Ryder A, et al. Stat5 promotes metastatic behavior of human prostate cancer cells *in vitro* and *in vivo*. Endocr Relat Cancer 2010;17:481–93.
6. Haddad BR, Gu L, Mirtti T, Dagvadorj A, Bajaj R, Vogiatzi P, et al. Stat5a/b gene locus undergoes amplification during human prostate cancer progression. Am J Pathol 2013;182:2264–2275.
7. Li H, Ahonen TJ, Alanen K, Xie J, LeBaron MJ, Pretlow TG, et al. Activation of signal transducer and activator of transcription 5 in human prostate cancer is associated with high histological grade. Cancer Res 2004;64:4774–82.
8. Li H, Zhang Y, Glass A, Zellweger T, Gehan E, Bubendorf L, et al. Activation of signal transducer and activator of transcription-5 in

prostate cancer predicts early recurrence. Clin Cancer Res 2005;11: 5863–8.
9. Thomas C, Zoubeidi A, Kuruma H, Fazli L, Lamoureux F, Beraldi E, et al. Transcription factor Stat5 knockdown enhances androgen receptor degradation and delays castration-resistant prostate cancer progression *in vivo*. Mol Cancer Ther 2010;10:347–59.
10. Casetti L, Martin-Lanneree S, Najjar I, Plo I, Auge S, Roy L, et al. Differential contributions of STAT5A and STAT5B to stress protection and tyrosine kinase inhibitor resistance of chronic myeloid leukemia stem/progenitor cells. Cancer Res 2013;73:2052–8.
11. de Groot RP, Raaijmakers JA, Lammers JW, Jove R, Koenderman L. STAT5 activation by BCR-Abl contributes to transformation of K562 leukemia cells. Blood 1999;94:1108–12.
12. Hoelbl A, Schuster C, Kovacic B, Zhu B, Wickre M, Hoelzl MA, et al. Stat5 is indispensable for the maintenance of bcr/abl-positive leukaemia. EMBO Mol Med 2010;2:98–110.
13. Horita M, Andreu EJ, Benito A, Arbona C, Sanz C, Benet I, et al. Blockade of the Bcr-Abl kinase activity induces apoptosis of chronic myelogenous leukemia cells by suppressing signal transducer and activator of transcription 5-dependent expression of Bcl-xL. J Exp Med 2000;191:977–84.
14. Lin TS, Mahajan S, Frank DA. STAT signaling in the pathogenesis and treatment of leukemias. Oncogene 2000;19:2496–504.
15. Nelson EA, Walker SR, Weisberg E, Bar-Natan M, Barrett R, Gashin LB, et al. The STAT5 inhibitor pimozide decreases survival of chronic myelogenous leukemia cells resistant to kinase inhibitors. Blood 2011;117:3421–9.
16. Nieborowska-Skorska M, Wasik MA, Slupianek A, Salomoni P, Kitamura T, Calabretta B, et al. Signal transducer and activator of transcription (STAT)5 activation by BCR/ABL is dependent on intact Src homology (SH)3 and SH2 domains of BCR/ABL and is required for leukemogenesis. J Exp Med 1999;189:1229–42.
17. Soliera AR, Mariani SA, Audia A, Lidonnici MR, Addya S, Ferrari-Amorotti G, et al. Gfi-1 inhibits proliferation and colony formation of p210BCR/ABL-expressing cells via transcriptional repression of STAT 5 and Mcl-1. Leukemia 2012;26:1555–63.
18. Warsch W, Kollmann K, Eckelhart E, Fajmann S, Cerny-Reiterer S, Holbl A, et al. High STAT5 levels mediate imatinib resistance and indicate disease progression in chronic myeloid leukemia. Blood 2011;117:3409–20.
19. Ye D, Wolff N, Li L, Zhang S, Ilaria RL Jr. STAT5 signaling is required for the efficient induction and maintenance of CML in mice. Blood 2006;107: 4917–25.
20. Ahonen TJ, Harkonen PL, Laine J, Rui H, Martikainen PM, Nevalainen MT. Prolactin is a survival factor for androgen-deprived rat dorsal and lateral prostate epithelium in organ culture. Endocrinology 1999;140: 5412–21.
21. Mirtti T, Leiby BE, Abdulghani J, Aaltonen E, Pavela M, Mamtani A, et al. Nuclear Stat5a/b predicts early recurrence and prostate cancer-specific death in patients treated by radical prostatectomy. Hum Pathol 2013;44:310–9.
22. Kazansky AV, Spencer DM, Greenberg NM. Activation of signal transducer and activator of transcription 5 is required for progression of autochthonous prostate cancer: evidence from the transgenic adenocarcinoma of the mouse prostate system. Cancer Res 2003;63:8757–62.
23. Tan SH, Dagvadorj A, Shen F, Gu L, Liao Z, Abdulghani J, et al. Transcription factor Stat5 synergizes with androgen receptor in prostate cancer cells. Cancer Res 2008;68:236–48.
24. Daley GQ, Van Etten RA, Baltimore D. Induction of chronic myelogenous leukemia in mice by the P210bcr/abl gene of the Philadelphia chromosome. Science 1990;247:824–30.
25. Gesbert F, Griffin JD. Bcr/Abl activates transcription of the Bcl-X gene through STAT5. Blood 2000;96:2269–76.
26. Savage DG, Antman KH. Imatinib mesylate—a new oral targeted therapy. N Engl J Med 2002;346:683–93.
27. Branford S, Rudzki Z, Walsh S, Grigg A, Arthur C, Taylor K, et al. High frequency of point mutations clustered within the adenosine triphosphate-binding region of BCR/ABL in patients with chronic myeloid leukemia or Ph-positive acute lymphoblastic leukemia who develop imatinib (STI571) resistance. Blood 2002;99:3472–5.
28. Gorre ME, Mohammed M, Ellwood K, Hsu N, Paquette R, Rao PN, et al. Clinical resistance to STI-571 cancer therapy caused by BCR-ABL gene mutation or amplification. Science 2001;293:876–80.
29. Levy DE, Darnell JE Jr. Stats: transcriptional control and biological impact. Nat Rev Mol Cell Biol 2002;3:651–62.
30. Becker S, Groner B, Muller CW. Three-dimensional structure of the Stat3-beta homodimer bound to DNA. Nature 1998;394:145–51.
31. Dagvadorj A, Collins S, Jomain JB, Abdulghani J, Karras J, Zellweger T, et al. Autocrine prolactin promotes prostate cancer cell growth via Janus kinase-2-signal transducer and activator of transcription-5a/b signaling pathway. Endocrinology 2007;148:3089–101.
32. Feldman L, Wang Y, Rhim JS, Bhattacharya N, Loda M, Sytkowski AJ. Erythropoietin stimulates growth and STAT5 phosphorylation in human prostate epithelial and prostate cancer cells. Prostate 2006;66:135–45.
33. Giri D, Ozen M, Ittmann M. Interleukin-6 is an autocrine growth factor in human prostate cancer. Am J Pathol 2001;159:2159–65.
34. Nevalainen MT, Valve EM, Ingleton PM, Nurmi M, Martikainen PM, Harkonen PL. Prolactin and prolactin receptors are expressed and functioning in human prostate. J Clin Invest 1997;99:618–27.
35. Hantschel O, Warsch W, Eckelhart E, Kaupe I, Grebien F, Wagner KU, et al. BCR-ABL uncouples canonical JAK2-STAT5 signaling in chronic myeloid leukemia. Nat Chem Biol 2012;8:285–93.
36. Neculai D, Neculai AM, Verrier S, Straub K, Klumpp K, Pfitzner E, et al. Structure of the unphosphorylated STAT5a dimer. J Biol Chem 2005; 280:40782–7.
37. Chen X, Vinkemeier U, Zhao Y, Jeruzalmi D, Darnell JE Jr, Kuriyan J. Crystal structure of a tyrosine phosphorylated STAT-1 dimer bound to DNA. Cell 1998;93:827–39.
38. Onishi M, Nosaka T, Misawa K, Mui AL, Gorman D, McMahon M, et al. Identification and characterization of a constitutively active STAT5 mutant that promotes cell proliferation. Mol Cell Biol 1998;18:3871–9.
39. Nevalainen MT, Harkonen PL, Valve EM, Ping W, Nurmi M, Martikainen PM. Hormone regulation of human prostate in organ culture. Cancer Res 1993;53:5199–207.
40. Berger A, Hoelbl-Kovacic A, Bourgeais J, Hoefling L, Warsch W, Grundschober E, et al. PAK-dependent STAT5 serine phosphorylation is required for BCR-ABL-induced leukemogenesis. Leukemia 2014;28:629–41.
41. Hedvat M, Huszar D, Herrmann A, Gozgit JM, Schroeder A, Sheehy A, et al. The JAK2 inhibitor AZD1480 potently blocks Stat3 signaling and oncogenesis in solid tumors. Cancer Cell 2009;16:487–97.
42. Muller J, Sperl B, Reindl W, Kiessling A, Berg T. Discovery of chromone-based inhibitors of the transcription factor STAT5. Chembiochem 2008;9:723–7.
43. Nam S, Scuto A, Yang F, Chen W, Park S, Yoo HS, et al. Indirubin derivatives induce apoptosis of chronic myelogenous leukemia cells involving inhibition of Stat5 signaling. Mol Oncol 2012;6:276–83.
44. Page BD, Khoury H, Laister RC, Fletcher S, Vellozo M, Manzoli A, et al. Small molecule STAT5-SH2 domain inhibitors exhibit potent antileukemia activity. J Med Chem 2012;55:1047–55.
45. Catane R, Kaufman JH, Nime FA, Evans JT, Mittelman A. Phase I study of N6-benzyladenosine-5'-monophosphate. Cancer Treat Rep 1978;62: 1371–3.
46. Hallek M. Chronic lymphocytic leukemia: 2013 update on diagnosis, risk stratification and treatment. Am J Hematol 2013;88:803–16.
47. Robak P, Robak T. Older and new purine nucleoside analogs for patients with acute leukemias. Cancer Treat Rev 2013;39:851–61.
48. Torella D, Curcio A, Gasparri C, Galuppo V, De Serio D, Surace FC, et al. Fludarabine prevents smooth muscle proliferation *in vitro* and neointimal hyperplasia *in vivo* through specific inhibition of STAT-1 activation. Am J Physiol Heart Circ Physiol 2007;292:H2935–43.
49. Goldman JM, Melo JV. Targeting the BCR-ABL tyrosine kinase in chronic myeloid leukemia. N Engl J Med 2001;344:1084–6.